UNIVERSITY OF GHANA

SCHOOL OF PHYSICAL AND MATHEMATICAL SCIENCES

UNDERSTANDING STOCHASTIC PROCESS FOR EQUATORIAL CLOUD PARAMETERIZATION IN REGCM4

BY

JOSHUA FAFANYO DZROBI

ID. NO. 10876665

A THESIS SUBMITTED TO THE SCHOOL OF GRADUATE STUDIES IN PARTIAL FULFILLMENT OF THE AWARD OF DEGREE OF MASTER OF PHILOSOPHY IN PHYSICS

DEPARTMENT OF PHYSICS

DECEMBER, 2022

DECLARATION

I, Mr Joshua Fafanyo Dzrobi (10876665), hereby declare that this work was carried out by me under the supervision of Prof. Nana Ama Browne Klutse, Dr. Nkrumah Francis and Dr. Azoda Hubert K. and that no previous submission on this topic has been made to this university or any other institution. Related works by others have been duly acknowledged by reference to authors.

……………………………………….. 24/10/2023 ……………………………..

JOSHUA FAFANYO DZROBI DATE

(STUDENT)

……….……………………………….. 25/10/2023 ……………………………..

PROF NANA AMA BROWNE KLUTSE DATE

(SUPERVISOR)

……………………………………….. 25/10/2023 ……………………………..

DR. NKRUMAH FRANCIS DATE

(CO. SUPERVISOR)

……………………………………….. 25/10/2023 ……………………………….

DR. AZODA HUBERT KOFFI DATE

(CO. SUPERVISOR)

ABSTRACT

Cloud parameterization is very essential in climate model because they represent weather quantities and processes that are extremely small or complex to be physically represented in climate models. The challenge of climate modelers to successfully and completely parameterize clouds reduces the confidence in climate simulations. In an attempt to improve climate simulations over West Africa, it has become indispensable to represent these uncertainties in the Regional Climate Model known as RegCM due to convective parameterizations. The performance and sensitivities of five (Emanuel, Grell, Tiedtke, Kain Fritsch and Betts Miller) convective schemes were evaluated against Climate Research Unit (CRU TS) observational data over a five year period (2010 - 2014) on a spatial resolution of 25km over the West African climatic sub-regions (Guinea coast, Savannah and Sahel regions). All simulations were forced with ERA-Interim reanalysis data. Precipitation and surface temperature were evaluated against CRU and relative humidity against ERA5 dataset for the seasons of December-January-February (DJF), March-April-May (MAM), June-July-August (JJA) and September-October-November (SON). This study observed a dominant wet bias for precipitation and relative humidity and warm bias for surface temperature. The wet (warm) bias for Emanuel (Grell) scheme significantly reduced over all sub-regions but the former outperformed the rest over the JJA analyses. The Emanuel scheme control parameters was stochastically perturbed to quantify uncertainties associated with convective cloud parameterization in simulating precipitation and surface temperature. The perturbed scheme improved the simulation of

precipitation but not surface temperature, even though the statistical skill of surface temperature were not degraded by the perturbations.

ACKNOWLEDGMENTS

I would like to express my heartfelt appreciation to Prof. Nana Ama Browne Klutse, Dr. Nkrumah Francis and Dr. Azoda Hubert K. for their respective contributions to make this work a success. I would also love to say a very big thank you to Mr. Graziano Giuliani of ICTP for his technical assistance, Dr Volker Kuell of University of Bonn, Mr. *Kuissi K. D.* Wilfried and Dr. Sekye Enock for their guidance. I would also like acknowledge and thank the African Institute of Mathematical Sciences (AIMS) Ghana for providing the funding that made this study a success. To God be the glory for this opportunity and the gift of these wonderful people in my life, I will forever remain grateful.

Table of Contents

Table of Figures

Index of Tables

CHAPTER ONE

1.0 INTRODUCTION

Understanding the climate and its complex interactions over a region was one of the motivations for developing regional climate models (RCM). After their first demonstration by Dickinson (1989) and Giorgi & Bates (1989), several efforts have been made over the years to improve their development, evaluation and applications in scientific research. The effectiveness of climate models in general is based, in part on the degree of a detailed description of the various physical processes represented. The other contributing factor is the spatial and temporal resolution at which the simulation is run. This is particularly important in regions where complex orographic effects and land use significantly affect the redistribution of climate variables (Wang et al., 2004). Regional climate modeling is also significantly important for scientific inquiry: understanding complex physical processes such as radiation feedback associated with clouds, topographic forcing, convection and many more can be refined by the use of RCMs (Sundqvist et al., 1989; Wang et al., 2004). This has been an active research area over the last few decades and great progress has been made. Some experts anticipate a future in which the feasibility of global circulation models (GCM) to be applied to a relatively "good" spatial resolution comparable to those currently used in RCMs would be possible. Some also argue that this future is skewed because GCM running at relatively "fine" spatial resolutions would require the parameterization of some physical processes; hence, the feasibility of this "golden future" will require the development of physical parameterization schemes for such high spatial resolution simulations as used in current RCM (Wang et al., 2004). This means that RCMs are indispensable even in the future. It is for this reason that experts suggest that the community of regional climate modelers can lead the way in the development of such physical parameterization schemes as is being done today. The credibility of RCMs in reproducing the variability of regional climate on different timescales is also well established in literature as demonstrated by Flatoy (1992); Goosse et al. (2010); and Wang et al. (2004). It is generally intuitive that despite the several feats accomplished since the introduction of the RCM, there still remain several challenges that confronts the community. One of such challenge is the long standing problems of physics parameterization in cumulus parameterization schemes.

1.1 Cumulus Parameterization Scheme

The public development of cumulus parameterization began somewhere in the 1960s by some of the leading authors including Charney & Elliassen, (1963). One key concern of cumulus parameterization schemes (CPS) has been the way and manner in which a detailed representation of atmospheric water vapor content in the atmosphere can be achieved in CPS (Emanuel, 1991; Emanuel & Živković-Rothman, 1999). This is rather an extremely important task because it reflects the very problem of cumulus parameterization especially when one is interested in precipitation processes. Cumulus parameterization began as an attempt to model tropical cyclones: parameterization became necessary in the absence of a self-consistent turbulent cumulus convective theory. This led to the use of convective adjustment of heat (temperature) profiles and water vapor as a replacement for the actual convective process (Arakawa, 2004). Convection is basically defined as the transport of heat and moisture by the movement of fluid typically from the surface of the earth up to the atmosphere. Clouds drive atmospheric weather conditions on a day to day basis and corollary climate conditions over a region over a longer timescale. The role of clouds in atmospheric dynamics has been well documented in literature (see Arakawa, (2004); Charney & Elliassen, (1963); Plant & Yano, (2015)). One key importance of clouds in atmospheric studies is that clouds modulate the earth's energy budget (see Figure 1.1). The modulation of the earth's energy budget by the sun is of extreme importance because this interactions basically drives atmospheric dynamics and affects almost all important variables such as atmospheric water content. Other very important effects of clouds on atmospheric dynamics are (see Jakob, (2003) for more):

1. Clouds directly or indirectly modify latent heat distribution as a result of phase changes of atmospheric water in clouds or convective precipitation.

2. Clouds significantly change surface hydrology profiles as a result of precipitation (rain or snow) produced by convective clouds.

3. Clouds change atmospheric dynamics by transporting momentum, moisture and heat over small and large spatial scales in convectively active regions.

Atmospheric water vapor content is an extremely important but a grossly difficult variable to account for in CPS. For studies interested in precipitation processes such as CPS, atmospheric micro-physics is of keen interest since all atmospheric dynamic theories will not be consistent without it. This statement describes the importance of microphysical considerations whenever atmospheric dynamics is being investigated. This has over the decades become one of the forefront problems of the cumulus parameterization community. Despite the importance of cloud microphysics in atmospheric dynamics, popular CPS have done very little to close this gap. Emanuel, (1991) and Emanuel & Živković-Rothman, (1999) comprehensively discussed the gravity of this neglect and the implications this can have on climate simulations. Every CPS seeks to accomplish some basic aims:

1. To account for the dynamics of latent heat and subsequent fluxes of momentum transport.

2. To reduce thermodynamic instability so that grid-scale precipitation and cloud parameterization (micro-physics) approaches do not attempt to generate unrealistic large-scale convection.

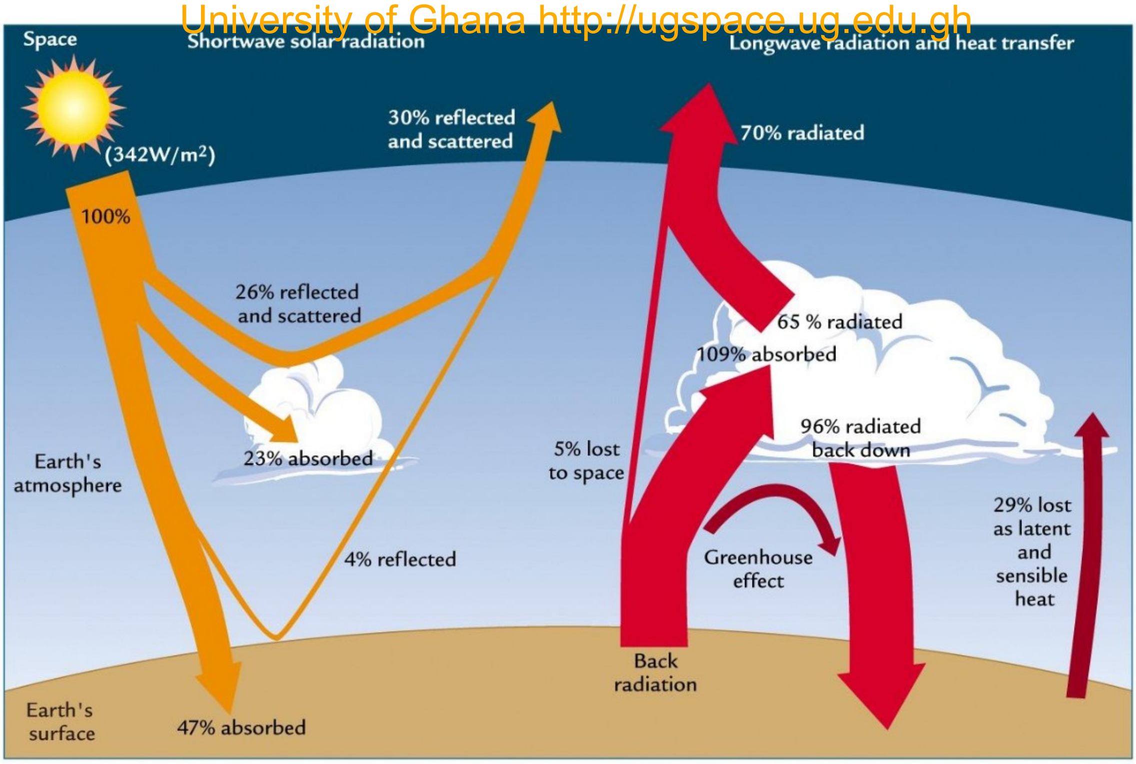

Figure 1.1: The effects clouds have on the earth's energy budget (Ruddman, 2000).

There are several ways of accomplishing the above stated aims and these stem from several tens of "cloud models" that have been formulated in the early years. "How should convective clouds be represented in atmospheric model?" is a question that still causes fierce contentions among experts. Each "cloud model" in an attempt to answer this question simply seeks to find a balance between mathematical simplicity, computational feasibility and physical consistency. Major contenders among these "cloud models" have been what is called the plume or thermal models (Blyth, 1993). A typical CPS in this regard consists of forming an ensemble out of a number of convective clouds within a grid box. Each cloud within this ensemble is averaged over its life cycle and its vertical structure is modeled as a plume and described in terms of its mass flux. Because of the complexity of convective systems, the interactions of the plume with its environment are restricted as much as possible to give a good physical account. The similar mathematical treatments stem from the similar assumptions made about both models: e.g., the rate of entraining air (along cloud edges) is proportional to vertical velocity and inversely proportional to cloud radius – this is further as a result of another assumption that velocity and buoyancy have the same horizontal distribution. Telford, (1975) later used this idea and made a complete model in which he introduced as a consequence the notion of parcels reaching equilibrium levels. He reasoned that density played a pivotal role in determining the level of equilibrium. The level of hydrostatic equilibrium he assumed to be between the cloud base and cloud top. This is the fundamental idea that several popular convective schemes of today are based on including Emanuel, (1991) and Emanuel & Živković-Rothman, (1999). Throughout literature, entrainment is said to play many pivotal roles in the formation, growth and dissipation of cumulus clouds. Entrainment is also known to decay the liquid water content of clouds. This is extremely undesirable for studies such as CPS which are interested in precipitating processes (Blyth, 1993). Parameterizing cumulus clouds comes with several difficulties that strongly correlates with major uncertainties, this is often grouped into two categories:

1. Structural and parameter uncertainties.
2. Inherent process uncertainties.

It must be understood here that these limitations in climate models is because cloud processes are not resolved and will not be in the near future hence are parameterized. This means that cloud processes do not have the luxury of real – world spatial and temporal variability hence the primary concern of every CPS is to attempt to represent as precise and accurately as possible, the microphysics of cloud processes, especially for precipitating cloud processes. Achieving this goal takes several methods and forms; popular of which are Convective Adjustment Schemes, and Mass-flux Schemes. The five (5) convective schemes used in this study fall under these broad categories.

1.1.1 Convective Adjustment Schemes (CAS)

The primary goal of the CAS is to ensure that the local vertical temperature and humidity in all forms remain physically realistic. These quantities are strongly constrained during both natural and forced convection hence the need to represent their individual contributions toward physical processes (Betts, 1986). The quasi-equilibrium state formed by deep convection can be represented directly. By doing this, CAS avoids errors that can occur when experimenting to estimate this state indirectly using increasingly sophisticated cloud models, the closure parameters of which can only be determined by comparing them to atmospheric observables (Betts et al., 1993). Betts-Miller (BM) is the only convective scheme used in this study that falls under this category. Following earlier theories, the concept of quasi-equilibrium between convective clouds and larger scale motions is now well established. This concept implies that convective zones have distinct temperature and moisture structures that may be observed and used as a foundation for convective adjustment. When there is shallow convection, the fluxes are designed to counteract the warming caused by large-scale sinking motion. The boundary layer structure will be skewed if these fluxes are not parameterized. For both deep precipitating and shallow non-precipitating convection, the scheme simultaneously adjusts the temperature (T) and moisture (q) profiles towards a quasi-equilibrium reference profile as:

$$\left(\frac{\partial \phi}{\partial t}\right)_{convection} = \frac{\phi_R - \phi}{\tau} \qquad (1.1)$$

where ϕ_R is the reference temperature, moisture and ϕ is the corresponding value of the grid point and τ is the adjustment timescales. The heat and moisture are subsequently implicitly redistributed by the convective adjustments defined by the equation 1.1. See (Betts, 1986) for further details.

1.1.2 Mass Flux Schemes

The bulk mass flux schemes are another attempt to understand and appropriately deduce how the complicated, nonlinear, and turbulent sub-grid processes contribute to the resolved grid flow of numerical weather prediction (NWP) models. Besides the CAS, another approach is to calculate the dynamic and thermodynamic tendencies from interactions from the environment and a simple 1D entraining plume and then average this over an area (Plant & Yano, 2015). This category of CPS has a number of difficulties which include the representation of entrainment, detrainment and the methods of invoking theoretical closures. Convection is represented in terms of environmental circumstances while precipitation is expressed in a grid-resolved variable in a microphysics scheme as much as possible. One of the great strengths of this approach of cloud parameterization is that it avoids the use of separate consideration to explicitly model each type of cloud that occurs in the ensemble including the cloud area and updraft velocity. Unfortunately, the advantage just stated also plays a role in the overall crude treatment of cloud microphysics, since several cloud characteristics and properties have to be considered at the same time for consistency. The microphysical representation of precipitation is considered reasonable by several authors including Emanuel, (1991); Emanuel & Živković-Rothman, (1999) who particularly criticized the scanty considerations of microphysical treatments in well known CPS. The contributions from convective updrafts, convective downdrafts, and the compensating sinking of the environmental air required to balance the mass flux moving up from convection are subdivided into vertical eddy transports:

$$\bar{\rho}_{cu}=\bar{\rho}\sum_{u} a_u\left(w_u-\bar{w}\right)\left(s_u-\bar{s}\right)+\rho\sum_{j} a_j\left(w_j-\bar{w}\right)\left(s_j-\bar{s}\right)+\bar{\rho}\left[1-\sum_{ij}\left(a_i-a_j\right)\right]\left(\tilde{w}-\bar{w}\right)\left(\tilde{s}-\bar{s}\right) \tag{1.2}$$

where **s** denotes dry static energy, **w** vertical velocity, **ρ** air density, and **q** specific humidity. The over-bar reflects the average over a large enough horizontal area to contain a cumulus cloud ensemble, whereas the prime represents deviations from the horizontal average. The subscript “**cu**” signifies convective contributions, the subscript “**u**” denotes cloud type, the subscripts “**i**” and “**j**” denote convective updrafts and downdrafts, respectively. The tilded denotes environmental air, and “**a**” denotes fractional area coverage. The average values for updrafts, downdrafts, and environmental subsidence (strong downdrafts) are used since it is considered that a one-dimensional model can properly describe their impacts. It is convenient to define the updraft (M_u) and downdraft (M_d) mass flux as

$$M_{ui}=\bar{\rho}\,a_{ui}\left(w_{ui}-\bar{w}\right) \tag{1.3}$$

$$M_{di}=\bar{\rho}\,a_{di}\left(w_{di}-\bar{w}\right) \tag{1.4}$$

The Kain-Fritsch, the Tiedtke, the Grell and the Emanuel convective schemes are all mass flux schemes.

1.1.3 The Kain-Fritsch Convective Scheme (KF)

Kain & Fritsch, (1990) proposes a cloud base mass flux method in which the amount of Convective Available Potential Energy (CAPE) in the environment that needs to be removed determines the cloud base mass flux. This may lead one to conclude that the strategy is based on deep-layer management, yet convection is activated through low level forcing. As a result, the Kain-Fritsch scheme is a low-level control scheme as well. The plan is also an instability-control technique because it concentrates on CAPE. One of the more complex trigger functions is also used in this system. In this method, shallow convection is not taken into account. Variable entrainment and detrainment rates are used in KF, which is based on the quality of updraft parcels that mix with the environment. The closure assumption determines how much updraft mass flux is required to remove CAPE. The cloud model contains a downdraft, but the downdraft is launched at an arbitrary height (~150200 hPa) above the cloud base and is fueled by the evaporation of condensate. According to parcel theory and an ingredient-based approach to understanding convection, the lifting of an air parcel from its Lifting Condensation Level (LCL) to its Level of Free Convection (LFC) determines when convection activates (Betts et al., 1993). The magnitude of the downdraft mass flux (M_d) at the top of the updraft source layer (USL) is described as a function of the updraft mass flux (M_u) and relative humidity inside the 150200 hPa layer of the downdraft source layer, such that;

$$Md_{USL} = -2\left(1 - \bar{RH}\right) Mu_{USL} \tag{1.5}$$

1.1.4 The Grell Convective Scheme

The cloud and environment are represented as two steady-state circulations in the Grell scheme (an undiluted updraft and a downdraft, i.e., no entrainment or detrainment occurs along the edges of the cloud, and the mass flux is constant with height). Because cloudy air and the environment are only mingled at the top and bottom of a raised parcel, the technique can be employed when it reaches moist convection level. The statistical equilibrium between large-scale processes and convection is the emphasis of this straightforward method. The minimum and highest levels of wet static energy dictate the downdraft and updraft initiating levels (Grell, 1993). The scheme takes the form;

$$M_d = \frac{\beta I_1}{I_2} M_u \tag{1.6}$$

I_1 and I_2 are representations of normalized updraft condensation and normalized downdraft evaporation, and β represents the fraction of updraft condensation that re-evaporates during the downdraft, which is dependent on the change in wind direction and speed, which normally varies between 0.3 and 0.5. Precipitation, P, can be calculated as;

$$P = I_1 m_b (1 - \beta) \tag{1.7}$$

The Grell scheme regulates the moistening, heating and the cooling impact during updrafts and downdrafts at the top and bottom of the cloud and this makes it very good for simulating relative humidity over the tropics. With a variety of assumptions, the Grell scheme is adaptable.

1.1.5 Tiedtke Convective Scheme

Tiedtke, (1989) considers convection to be dependent on moisture supply from large-scale moisture convergence and boundary layer turbulence, making this scheme a moisture-control scheme as well. The plume entrainment rate of the model, which is used to represent convective clouds, is affected by the amount of large-scale convergence, with lower values of entrainment when large-scale convergence is present. This assumption causes the updraft entrainment to be divided into two terms: one approximating the turbulent exchange of mass at the cloud edges (E^1_u), and the other representing the organized inflow into the cloud from large-scale convergence (E^2_u). A similar assumption is made for detrainment (D_u), which results in the relationships:

$$E_u = E_u^1 + E_u^2 \tag{1.8}$$

$$D_u = D_u^1 + D_u^2 \tag{1.9}$$

A lower entrainment rate generally results in deeper clouds, so deep convection is more likely in this scheme in the presence of large-scale flow convergence. Tiedtke, (1989) concludes the scheme by referring back to Kuo, (1965) study that established a relationship between convective activity and large-scale moisture convergence. As a result of this assumption, the low-level sub-cloud layer is subjected to a moisture balance, and cloud mass flux is clearly linked to low-level, large-scale moisture convergence. This relationship is defined as follows:

$$\left[M_u\left(q_u-\bar{q}\right)+M_d\left(q_d-\bar{q}\right)\right]_{cb}=-\int_0^{cb}\left(\vec{\bar{V}}\,.\,\nabla\bar{q}+\bar{w}\frac{\partial\bar{q}}{\partial z}+\left(\bar{\rho}\,\bar{w}'\bar{q}'\right)_{pbl}\right)\bar{\rho}\,dz \qquad (1.10)$$

The subscript cb stands for cloud base. One can calculate the relative downdraft mass flux at the cloud base from a small initial cloud base updraft mass flux, and so iterate to determine the required amount of updraft mass flux at the cloud base to match the large-scale moisture convergence in the sub-cloud layer. The scheme incorporates shallow convection, with shallow clouds detraining at both their neutral buoyancy level and the model level above it.

1.1.6 Emanuel Convective Scheme

Rather than a continuous mixing, the buoyancy sorting method assumes mixing of cloudy air and environmental air to be highly episodic and inhomogeneous. Air from the environment entrains into a cloud and mixes with the cloud in different fractions (inhomogeneous) hence the different fractions of mixtures will have different buoyancies due to different densities and temperatures profiles. These different mixtures then descend to their respective level of neutral buoyancy. Emanuel & Živković-Rothman, (1999) argued that the entraining plume model that has been employed over decades in the CPS community has become outdated and inconsistent with observational results. Laboratory work on entraining plumes strongly indicates the dependence of the entraining and detraining rates (mixing rates) on mean upward vertical velocity but penetrative convection obviously modifies the mixing rate. The author however formulates the rate of entrainment and detrainment on the assumption that the rates of mixing depended strongly on the vertical gradient of buoyancy in clouds. Increasing buoyancy with height enhances entrainment while decreasing buoyancy enhances detrainment. The fraction of total cloud base mass flux (M_b) that mixes with its environment at any level is:

$$\delta M = M_b \times \frac{|\delta B| + \wedge\, \delta p}{\sum_{i=1}^{N} \left[|\delta B| + \wedge\, \delta p \right]} \tag{1.11}$$

Where δB is the undiluted buoyancy gradient over pressure interval δp, Λ is a mixing parameter and N is the number of model levels. The absolute value of buoyancy above translates as: either increases the rate of mixing δM. Equation 1.11 allows cloud base mass flux to adjust to cloud buoyancy variations hence driving the system to quasi-equilibrium. The scheme uses a uniform probability density function (PDF) for all mixing. Many authors have criticized the use of such a simple PDF, it is certain that the use of this PDF limits possibilities. Grandpeix et al., (2004) for example replaced the uniform PDF with a two parameter bell shaped function that allows a wider range of behaviors. Emanuel used subcloud layer quasi-equilibrium hypothesis (see Emanuel, (1991); Emanuel & Živković-Rothman, (1999) for more details) as;

$$\frac{\partial M_b}{\partial t} = \frac{\alpha}{\Delta t} \left(T_{(\rho p)} - T_\rho + \Delta T_k \right)_{LCL} - \frac{D}{\Delta t} M_b \tag{1.12}$$

where $T_{(\rho p)}$ is the density temperature of the parcel lifted adiabatically from the subcloud layer, T_ρ is the density temperature of the environment, α is a fixed parameter, Δt is the time step and D is a damping effect. Following the equation 1.12, one principally important concern is the precipitation efficiency thus how much condensed cloud water was converted to precipitation. This concern is paramount because the remaining is going to be responsible for moistening the environment. Emanuel adopts the philosophy of converting all cloud water in excess of a threshold content (l_c) to precipitation within each sample of cloud air. By this adoption, Emanuel accounts for ice processes rather crudely by allowing l_c to be temperature dependent. While admitting the crude nature of this considerations, it should be noted that not even one of the 3 mostly widely used convective schemes made any such attempts to account for the non-linearity of stochastic coalescence (ice processes). Emanuel & Živković-Rothman, (1999) adds precipitation to a single hydrostatic unsaturated downdrafts that transports heat and water, as well as allow the evaporation of this precipitation to be described by a standard rate equation. Deep convective downdrafts has significant impacts on surface fluxes. The deep convective downdraft velocity scale w_d is defined as;

$$|\bar{V}| = \sqrt{|V^2| + u^2 + w_d^2} \tag{1.13}$$

where $|\bar{V}|$ is the grid box-average surface wind speed, u is the dry turbulent boundary layer velocity scale. The unsaturated downdraft mass flux M_d is taken to be proportional to w_d as defined by;

$$w_d = \frac{\beta M_d}{\rho \sigma_d} \tag{1.14}$$

where ρ is the air density, σ_d is the fractional area covered by convective downdraft and β is a constant parameter. The convective scheme works by checking each model level for instability to upward displacement hence the importance of buoyancy profile. The model considers convection to occur only at the first level that is unstable to upward displacement. It is considered based on observational evidence that elevated convection can only occur when the boundary layer is distinctly stable. The current Emanuel scheme (Emanuel, (1991); Emanuel & Živković-Rothman, (1999)) cannot simulate the shallow/deep convection regime transition because the cloud-top height in this parameterization is entirely determined by adiabatic ascent of the undiluted updrafts. This can be faulty in most cases and constitutes a weakness of the scheme (Grandpeix et al., 2004).

1.2 PROBLEM STATEMENT

The emphasis on the importance of cumulus parameterization can arguably not be made any more than is documented in literature (Jakob 2003;Of 2004; Wang 2004; Deshpande 2012). Clouds and cloud processes are not resolved by RCM, this means that they lack the luxury of the real world spatial and temporal variability. This is an enormous problem because cloud processes significantly affect atmospheric dynamics such that they cannot be ignored. CPS hence have a responsibility for representing these processes in the best and precise way as possible. This is usually a difficult task for CPS for a number of reasons, one of which is that; one of the major sources of errors associated with CPS is structural and parameter uncertainties. The difficulties stem from the fact that control parameters of CPS such as those of the bulk mass flux schemes define the theoretical basis on which the closure, the trigger function and the mixing rate of cloudy and environmental air is defined. More important and practical is that these control parameters depends on the exact shape and configuration of the cloud, and this is extremely difficult to determine. Stochastic perturbations have been be argued as a remedy for this problem.

1.3 PURPOSE OF STUDY

The purpose of this study is to explore the sensitivity of five (5) convective parameterization schemes with the new surface scheme CLM version 4.5 tailing only the study by Koné et al. 2018. The most effective scheme in simulating precipitation will have its control parameters perturbed using stochastic perturbations.

1.4 OBJECTIVE OF STUDY

This research aims to improve the conventional convective parametrization scheme that produces the most realistic simulation of precipitation by employing stochastic perturbations.

1.5 SUB-OBJECTIVES OF STUDY

The sub-objectives of this study are:

1. To investigate the sensitivity of convective schemes over the West African domain in RegCM4.7.1.

2. Subject convective scheme parameters of the Emanuel convective scheme to stochastic perturbations in RegCM4.7.1.

3. Assess the impact of perturbed Emanuel convective scheme on climate variables in RegCM4.7.1.

1.6 ARRANGEMENT OF WORK

This study is arranged in the following order: Chapter One contains an introduction to the subject matter. Chapter Two contains a review of literature specific to the model and relevant information about the model. Chapter Three contains the methodology employed and data description. Chapter Four contains results and discussions. Chapter Five contains conclusions and recommendations for future research.

CHAPTER TWO

2.0 LITERATURE REVIEW

2.1 Empirical Literature

There has been a lot of work in the past to test the sensitivity of existing CPS over many different regions and over various vertical and horizontal spatial and temporal resolutions. Unfortunately most of these studies are over regions other than the West African region. This is what this study attempts to remedy. The importance of convection, particularly moist convection in understanding climate dynamics and evolution has been well established by thorough discussions including Emanuel (1991); Emanuel & Živković-Rothman (1999); Adeniyi (2014); Deshpande et al. (2012); Komkoua Mbienda et al. (2021); Koné et al. (2018) and Raymond (1956). Earlier research such as Meinke et al., (2007) has already established that the West African Monsoon precipitation is sensitive to the type of cumulus parameterization scheme hence the need to evaluate available convective schemes over the region. Adeniyi, (2014) used the ICTP RegCM4.0 to simulate the West African climate. In this study, the author test the sensitivity of the Grell, Kuo and Emanuel convective schemes for September of 1989 and 1998 because they succeeded a strong La Nina and El Nino respectively. Adeniyi, (2014) reported good performance of the various convective schemes in capturing the various climatic dynamics including the dynamics of the inter-tropical convergence zones. Kuo was reported to have produced the highest precipitation bias as compared to CRU and GPCP observational projects. The performance of the Grell CPS depended on the closure scheme used, for example, Grell with Arakawa-Schubert (Grell1) closure underestimated precipitation during the study as compared to Grell with Fritsch Chappel (Grell 2) closure. This is one of the many instances in which the use of different closure assumptions for the same scheme produces different results. For the period and duration of study, Grell 2 outperformed the rest of the CPSs in simulating large scale precipitation but also joined the rest in their failure to simulate the regional distinction between the 1989 and 1998 September total precipitation. Precipitation over the West Africa region is greatly influenced by the Atlantic Ocean. The intensity of rainfall around mountains is also well documented. South westerly winds from the Atlantic Ocean are forced up by the mountains hence accelerating precipitation processes. This is an important dynamic in simulating precipitation in West Africa and Adeniyi, (2014) among other things observed that Grell1, Grell2 and Kuo captured this dynamic properly whiles Emanuel does not. This maybe attributed to how Emanuel convective scheme generally triggers convection when the level of neutral buoyancy is higher than the cloud-base level. When air is lifted between these two levels, a fraction of the condensed moisture forms precipitation while the remaining fraction forms a cloud. This does not give the freedom to account for mountain perturbations (Komkoua Mbienda et al., 2021). Kouassi et al., (2022) assessed the performance of two land surface models (BATS and CLM 4.5) over the West African region. He concluded that the temporal localization (seasonal effect), spatial distribution (grid points) and magnitude of precipitation and temperature (bias) are not enhanced by the CLM4.5. Even though both land surface schemes improve the statistical performance of the model, the BATS land surface scheme is relatively old but outperforms the new CLM 4.5 particularly in the Sahel region. CLM 4.5 also fails drastically in reducing the air surface temperature in the Sahel and Sahara regions. Kouassi et al., (2022) however failed to discuss how the various convective schemes improve or deteriorate the performance of land surface schemes that were the center of his work. Komkoua Mbienda et al., (2021) assessed the performance of ten convective schemes over East Africa and discussed their ability to simulate key climate features in the study area. One key conclusion that can be drawn from this study is that there is no best convective scheme to represent both precipitation and surface temperature. This in a way contradicts the work of Koné et al., (2018) who recommended that the Emanuel convective scheme is suitable for the simulation of precipitation and surface temperature over West Africa. This not-withstanding, it is important to mention that Komkoua Mbienda et al., (2021) stressed that the choice of an appropriate convective scheme are strictly related to the season, study year and version of the RegCM used. Emanuel convective scheme has been primarily outstanding in simulating precipitation and to a lesser extent, surface temperature and this may be due to the unique and physically appropriate trigger function the scheme uses (Komkoua Mbienda et al., 2021; Koné et al., 2018; Kouassi et al., 2022). Besides the work of Kouassi et al., (2022), no other have employed the new community land model (CLM 4.5) in assessing the sensitivity of this configuration of RegCM (with CLM 4.5 rather than BATS) to convective schemes over West Africa but Koné et al., (2018). In this study, Koné et al., (2018) employed three convective scheme: Emanuel, Grell, and Tiedtke and two mixtures of Grell and Emanuel over land and ocean. Emanuel was recommended by this study for West African climate studies. Other numerous sensitivity studies have been conducted over other parts of the globe to test the version of RegCM and physics configuration that works best (see Ali et al., (2015); Raj Tiwari et al., (2015) for more). There have been recent concerns about the use of models particularly regional climate models as a "black-box" and without real care about optimizing or investigating the behavior of these cumulus scheme upon perturbing the scheme parameters and this is one of the objectives of this work.

2.2 The RegCM4.7.1 Model

The model used in this study is the International Center for Theoretical Physics (ICTP) Regional Climate Model version 4.7.1 (RegCM4.7.1). Its development started in the late 1980s. For more information (Elguindi et al., (2006, 2011); Giorgi et al., (2016)). It has since been maintained and improved to RegCM2 (Giorgi et al., 1993), RegCM3 (Pal et al., 2007), and RegCM4 (Elguindi et al., 2006; Pal et al., 2007). The Earth System Physics (ESP) group at the ICTP in Italy maintains the model. The RegCM4.7.1 is a limited area model with finite-difference discretization using a terrain–following a sigma (σ) pressure vertical coordinate system. RegCM4 was developed to study mesoscale processes in the atmosphere over a selected domain. A hydrostatic dynamical core of the mesoscale model version 4 (MM4) and uses the Holtslag planetary boundary layer scheme (Holtslag, 1990) which is formulated to calculate turbulent transportation of water vapor, sensible heat and momentum in the planetary boundary layer over land and ocean is employed by the model.

Counter-gradient fluxes are also accounted for but as a consequence of non-local transport in the convective boundary layer. The scheme produces relatively strong and often excessive, a turbulent vertical transfer which can among other things result in low moisture amounts near the surface and excessive moisture near the PBL top. The model corrected this by removing the counter-gradient term for water vapor (Elguindi et al., 2011). In addition to the convective parameterization schemes employed, the large-scale precipitation scheme of Pal et al., (2000) referred to as the SUBgrid EXplicit moisture scheme (SUBEX), includes the sub-grid variability in clouds (Sundqvist et al., 1989) and the evaporation and accretion processes for stable precipitation. The soil, vegetation and atmosphere interaction processes are parameterized using Community Land Model (Elguindi et al., 2011). CLM4.5 presents in each grid cell the possibility to have 15 soil layers, five different land unit types and 16 different plant functional types. RegCM4-CLM4.5 proposes five different convective schemes (Elguindi et al., 2011): the Tiedtke scheme (Tiedtke, 1989), the Emanuel scheme (Emanuel, 1991; Emanuel & Živković-Rothman, 1999), the Grell scheme (Grell, 1993) and the Kain–Fritsch scheme (Kain & Fritsch, 1990; Of et al., 2004). It also includes many complex detailed processes such as, radiative transfer processes, grid-scale and subgrid-scale cloud processes, turbulence mixing processes and land-surface processes. RegCM4.7.1 and other newer versions shows an improvement in performance as well as are more user-friendly, versatile and portable compared to the older version especially in the formulation of surface scheme. The RegCM4.7.1 has over the period demonstrated unprecedented flexibility, high resolution and performance over the African continent (Browne, 2012; Adeniyi, 2014; Klutse, 2016; Ogwang, 2016; Kouassi, 2022; Kouassi, 2022). The flexibility, fine resolution and unprecedented performance has made the RegCM4.7.1 popular in the study of past, present and future climate dynamics particularly dynamics of the West African climate. The present study does not only aim at assessing the sensitivity of convective schemes but also to improve convective parameterization scheme by employing stochastic perturbations. This will be accomplished by assessing precipitation, surface temperature and relative humidity. These climatic variables are closely tied to the dynamics of the West African Monsoon (WAM). The RegCM4.7.1 have shown skilled and great performance in understanding the dynamics of the WAM as demonstrated by Browne, (2012); Adeniyi, (2014); Klutse, (2016); Ogwang, (2016); Kouassi, (2022); Kouassi, (2022). These reasons has made the RegCM4.7.1 a model of choice considering the climatic variables of interest (precipitation, surface temperature and relative humidity) in this study.

2.2.1 Model Equations

The RegCM model solves a set of primitive dynamical equations that describe atmospheric motion, with physical processes parameterized to provide a bulk effect of sub-grid processes such as planetary boundary layer. The model is traditionally composed of three (3) dynamical cores:

1. Hydrostatic equation solver
2. Non-hydrostatic equation solver with pressure coordinate
3. Non-hydrostatic equation solver with height coordinate

2.2.2 Hydrostatic Equation Solver.

This study makes use of the hydrostatic dynamical core prepared based on hydrostatic model dynamic equations and numerical discretization as described in details by Grell et al., (1995). Equations 2.1 and 2.2 are a few important equations and relations that best describe momentum and thermodynamical model equations.

$$\frac{\partial \tilde{p} u}{\partial t} = -m^2\left[\frac{\partial \tilde{p} u u/m}{\partial x} + \frac{\partial \tilde{p} v u/m}{\partial y}\right] - \frac{\partial \tilde{p} u \dot{\sigma}}{\partial \sigma} - m\tilde{p}\left[\frac{\sigma}{\rho}\frac{\partial \tilde{p}}{\partial x} + \frac{\partial \phi}{\partial x}\right] + \tilde{p} f v + F_H u + F_V u \quad (2.1)$$

$$\frac{\partial \tilde{p} v}{\partial t} = -m^2\left[\frac{\partial \tilde{p} u v/m}{\partial x} + \frac{\partial \tilde{p} v v/m}{\partial y}\right] - \frac{\partial \tilde{p} v \dot{\sigma}}{\partial \sigma} - m\tilde{p}\left[\frac{\sigma}{\rho}\frac{\partial \tilde{p}}{\partial y} + \frac{\partial \phi}{\partial y}\right] + \tilde{p} f u + F_H v + F_V v \quad (2.2)$$

where $\bar{p} = p_s - p_t$ with p_s and p_t corresponding to surface pressure and pressure top of the model. The eastward and northward velocity components are represented as "u" and "v", ϕ is the geopotential height, "f" is the Coriolis parameter, "m" is the map scale factor for the chosen projection. The F_H and F_V represent the horizontal and vertical diffusion terms.

$\dot{\sigma}$ is also described as $\dot{\sigma}=\frac{d\sigma}{dt}$, where σ is the vertical coordinate.

$\frac{\sigma}{\rho}=\frac{RT_v}{(\tilde{p}+p_t/\sigma)}$ and the $T_v=T(1+0.608q_v)$is the relation for the virtual temperature. “T” and “R” are also temperature and gas constant of dry air respectively.

2.2.3 Continuity Equations

The surface pressure is computed from the continuity equations as:

$$\frac{\partial\tilde{p}}{\partial t}=-m^2\left[\frac{\partial\tilde{p}u/m}{\partial x}+\frac{\partial\tilde{p}v/m}{\partial y}\right]-\frac{\partial\tilde{p}\dot{\sigma}}{\partial\sigma} \qquad (2.3)$$

The temporal variation of the surface pressure in the model can be computed from the vertical integration of equation (2.3):

$$\frac{\partial\tilde{p}}{\partial t}=-m^2\int_0^1\left[\frac{\partial\tilde{p}u/m}{\partial x}+\frac{\partial\tilde{p}v/m}{\partial y}\right]d\sigma \qquad (2.4)$$

At this point, the vertical velocity at each level of the model in sigma coordinates can now be obtained by employing the surface pressure tendency from equation (2.4).

$$\dot{\sigma}=-\frac{1}{\tilde{p}}\int_0^{\sigma}\left[\frac{\partial\tilde{p}}{\partial t}+m^2\left(\frac{\partial\tilde{p}u/m}{\partial x}+\frac{\partial\tilde{p}v/m}{\partial y}\right)\right]d\sigma' \qquad (2.5)$$

where σ’ is the dummy variable of integration and $\dot{\sigma}(\sigma=0)=0,\dot{\sigma}(\sigma=1)=0$.

2.2.4 Thermodynamic equations

The thermodynamic equations begin as:

$$\frac{\partial\tilde{p}T}{\partial t}=-m^2\left[\frac{\partial\tilde{p}uT/m}{\partial x}+\frac{\partial\tilde{p}vT/m}{\partial y}\right]-\frac{\partial\tilde{p}T\dot{\sigma}}{\partial\sigma}+\frac{RT_v\omega}{c_p(\sigma+p_t/\tilde{p})}+\frac{\tilde{p}q}{c_p}+F_HT+F_vT \qquad (2.6)$$

c_p can be calculated once the heat capacity of dry air (c_{pd}) and the water vapor mixing ratio (q_v) are known: $c_p=c_{pd}(1+0.8q_v)$

c_{pd} is the specific heat capacity for the moist air at constant pressure, Q is the adiabatic heating, $F_H T$ and $F_V T$ are the horizontal diffusion effects and the effects of vertical mixing and dry convective adjustment. Whiles $\omega=\frac{dp}{dt}=\tilde{p}\dot{\sigma}+\sigma\frac{d\tilde{p}}{dt}$ and $\frac{d\tilde{p}}{dt}=\frac{\partial\tilde{p}}{\partial t}+m\left[u\frac{\partial\tilde{p}}{\partial x}+v\frac{\partial\tilde{p}}{\partial y}\right]$

The hydrostatic equations can now be used to compute the geopotential heights from the virtual temperature.

$$\frac{\partial\phi}{\partial\ln\left(\sigma+p_t/\tilde{p}\right)}=-RT_v\left[1+\frac{\sum q_x}{\left(1+q_v\right)}\right]^{-1} \qquad (2.7)$$

It becomes theoretically necessary to linearized these equations, hence we defined a state such that:

$$\bar{u}=0$$
$$\bar{v}=0$$
$$T=\bar{T}$$
$$f_0=\bar{f}$$
$$\tilde{p}=\bar{p}$$

This rest state is used to linearize the equations.

2.3 Physics Parameterizations

This section describes briefly the various parameterization schemes that the model utilizes. The land surface scheme and the PBL scheme will be explained in the later paragraphs in addition to the convective parameterization schemes that have been explained in the previous chapter. The radiation scheme used in the RegCM4 is the one of the NCAR CCM3. The scheme accounts for the effects of major gases such as water (H_2O), oxygen (O_2), and carbon dioxide (CO_2) based on δ-Eddington approximation. The cloud scattering and absorption parameterizations include 18 spectral intervals and are based on the work by Slingo, (1988). Here, the optical properties of clouds such as optical depth are described in terms of the cloud's liquid water content among other things. This description is convenient for the microphysical considerations of cloud processes. The total cloud cover at a grid-point in a model column (from cloud-base to cloud-top) is a function of the horizontal grid-point spacing while the thickness of the cloud layer is assumed to be equal to that of the model layer.

2.4 Land Surface Scheme

The land surface and its interactions with the rest of the atmosphere are parameterized. There are basically two land-surface schemes; the Biosphere -Atmosphere Transfer Scheme (BATS) and the Community Land Model scheme (CLM). The BATS is the default scheme but this study utilized CLM version 4.5, designed to describe the role of vegetation and interactive soil moisture in modifying the surface-atmosphere exchanges of momentum, energy, and water vapor. The CLM scheme provides more details compared to the BATS. The scheme defines explicitly the solutions of temperature and water (liquid and ice) in ten unevenly spaced soil layers. The complexity of land surface interactions is explicitly accounted for by employing the “mosaic” approach to capture surface heterogeneity. The grid cell of every CLM contains up to four different land cover types such as glaciers, wetlands, vegetated land and lakes. The vegetated land is further divided into seventeen types to account for the various vegetation covers. This is extremely important in this study regarding the nature of the topography of the study area.

The CLM scheme was first developed for global circulation models (GCM) hence it was readjusted for implementation into the RegCM infrastructure. This means that the scheme would require high-resolution input data such as land cover for initialization. The fine resolution requirement of the input parameters is to help capture as much as possible surface heterogeneity (refer to Elguindi et al., (2011) for more information).

2.5 Planetary Boundary Layer Scheme

The behavior and properties of the PBL is another key process to be accounted for during the simulation of weather and climate patterns. This account is captured by parameterizing the processes, and interactions of the PBL since it is also a subgrid process. The study employs the Holtslag PBL scheme. As mentioned briefly above, the scheme is constructed on the theory of non-local diffusion that is based on counter-gradient fluxes that results from large-scale eddies in an unstable but well mixed atmosphere. The scheme defines vertical eddy flux within the PBL as

$$F_c = -K_c\left(\frac{\partial C}{\partial z} - \gamma_c\right) \qquad (2.8)$$

The terms are defined as; K_c is the eddy diffusivity, C is a constant whose value is 8.5 (Elguindi et al., 2011), and γ_c is a counter-gradient transport term that describes non-local transport owing to dry deep convection. This transport term is important in convective environments and its definition is dependent on climatic variable being considered. In terms of temperature and water vapor,

$$\gamma_c = C\left(\frac{\phi_c}{\omega_t h}\right) \qquad (2.9)$$

In calculating the non-local transport term, one will require the temperature or water vapor flux within the boundary layer (ϕ_c), its value is assumed to be zero if otherwise (and for momentum considerations). "ω_t" is the turbulent convective velocity is strongly dependent on the friction velocity, "h" is the height of the boundary layer defined and elaborated on in Elguindi et al., (2011).

2.6 Large-Scale Precipitation Scheme

The model used in this study resolves some precipitation processes and non-convective clouds, this is captured by the Subgrid Explicit Moisture Scheme (SUBEX). It becomes important to account for subgrid variability that drives this processes. Basically SUBEX does that by linking the average grid cell relative humidity to the cloud water and cloud fraction and is mainly based on the work of Sundqvist et al., (1989). The grid cell cloud fraction is given by

$$CF = \sqrt{\frac{RH - RH_{min}}{RH_{max} - RH_{min}}} \qquad (2.10)$$

The RH_{min} parameter here is the minimum relative humidity threshold at which clouds begin to form, RH_{max} is the relative humidity value where CF reaches unity. CF is convincingly assumed to be zero when RH < RH_{min} and unity when RH > RH_{max}. Precipitation forms when the cloud water content exceeds the auto-conversion threshold "l_c^{th}" according to

$$P=C\left(\frac{l_c}{CF-l_c^{th}}\right)CF \qquad (2.11)$$

"P" here refers to precipitation, the inverse of "C" (1/C) describes the characteristic time for which cloud droplets are converted to raindrops. Precipitation here is allowed to fall instantaneously. The auto-conversion threshold is obtained here by having the median cloud liquid water content equation scaled as elaborated in Elguindi et al., (2011).

2.7 Cloud Micro-Physics Scheme

As mentioned earlier, cloud microphysics is very crucial in the effective description of convection and convective forcing and processes which leads to the formation of precipitation among others. Of all five (5) schemes used in this study, only the Emanuel scheme crudely accounts for cloud microphysics. To enhance this deficiency, the model includes a cloud microphysics scheme which is built upon the European Center for Medium Weather Forecast's (ECMWF) Integrated Forecast System (IFS). The new scheme solves equations for prognostic variables such as water vapor content, cloud liquid water, rain. The equation for each variable can be written in the form:

$$\frac{\partial q_x}{\partial t}=S_x+\frac{1}{\rho}\frac{\partial}{\partial z}\left(\rho V_x q_x\right) \qquad (2.12)$$

The local variation of the mixing ratio, "q_x" of the variable "x" is given by the sum of microphysical sources and sinks (condensation, evaporation, auto-conversion) of "q_x" (S_x) and the sedimentation term which happens to be a function of the fall velocity V_x and density ρ. The microphysical sources and sinks are divided into two groups depending on the transient nature of the process they represent. All fast occurring processes (relative to the timestep) are treated implicitly while slow occurring processes are explicitly described. The scheme also makes good attempts to achieve some commendable features:

i. The scheme successfully allowed the existence of supercooled liquid water by making liquid water independent of icy water. As a consequence, the scheme is able to represent the mixed phase cloud systems as observed.

ii. The advection of rain and snow was also achieved by allowing precipitation (rain, snow) to fall with a fixed, finite, terminal velocity.

iii. The scheme is designed to periodically check for the conservation of total moisture and enthalpy.

As mentioned, microphysical processes lead to the release or the absorption of latent heat energy (sources and sinks). This perturbs the temperature budget significantly enough that it becomes necessary to account for (Elguindi et al., 2011).

CHAPTER THREE

3.0 EXPERIMENTAL METHOD

This research aims to improve conventional convective parametrization by employing stochastic perturbations. This is expected to estimate uncertainties introduced into climate simulations and to capture more appropriately the response of climate simulations to changes in external forcing which has a huge impact on the prediction of precipitation and relative humidity. Figure 3.1 briefly describes the methodology employed in designing, running and analyzing results from the climate simulations over West Africa. This study relies on the “SURFACE files” for precipitation and surface temperature (2m - temperature) whiles the relative humidity variable was extracted from the “ATMOSPHERE file” produced by the model simulation. The model was forced with Global Circulation Model (GCM) ERA-Interim (ERA15) datasets. ERA15 used in this study contained comprehensive climate variables including wind, humidity, temperature. Table 3.4 summarizes the main model properties. The main statistical parameters were calculated using equations 3.1 to 3.4. The model domain of this study is the West African region which can be found between longitude 20W to 20E and latitude 5S to 21N. The model used is the RegCM 4.7.1 developed and maintained by the ICTP (Elguindi et al., 2011). The West African region is basically divided into three characteristic climatic sub-regions: the Guinean zone (20W:20E, 4N:8N), Savannah zone (20W:20E, 8N:12N), and Sahel zone (20W:20E, 12N:16N) as shown in Figure 3.1. For this study, the model was run with 23 vertical sigma layers with the model top at 100 hPa (10cbar) and builds initial and boundary conditions for the regional scale, interpolating on the RegCM grid the data from GCM. The study was divided into two main parts:

a. Investigate the sensitivity of conventional convective parameterization schemes with respect to precipitation, surface temperature and relative humidity simulations.

b. Subject convective scheme parameters to stochastic perturbations.

3.1 Sensitivity Experiments

All simulations in this section are similar in all aspects of the model setup except for the convective scheme (over land and ocean). The study focused on precipitation, surface temperature and relative humidity over a five (5) year period (2010 to 2014) and validates the results of the simulations for December-January-February (DJF), March-April-May (MAM), June-July-August (JJA) and September-October-November (SON) over West Africa (WA), Guinea coast (GC), Savannah region (Sav) and the Sahel region (Sah). CRU TS4 and ERA5 were used to validate the results from the simulation. To measure the quantitative skill of the model (convective schemes), we consider the following cost functions (comparison metrics): mean bias (MB), which is the difference between the area-averaged value of the simulation and the observation – an indication of the sensitivity, hence the accuracy of the CPS as compared to observation, the spatial root mean square error (RMSE) – an indication of the magnitude and weighted error between the CPS and observation, the pattern correlation coefficient (PCC) – an indication of spatial consistency and agreement between CPS and observation. The RMSE, and PCC provide information at the grid-point level, while the MB does so at the regional level.

$$RMSE=\sqrt{\frac{1}{n}\sum_{i=1}^{n}e_i^2} \tag{3.1}$$

$$Correleration(PCC)=\frac{\sum_{i=1}^{n}(s_i-\mu_s)(o_i-\mu_o)}{\sqrt{\sum_{i=1}^{n}(s_i-\mu_s)^2(o_i-\mu_o)^2}} \tag{3.2}$$

$$Mean\,Bias=\frac{1}{n}\sum_{i=1}^{n}e_i^2 \tag{3.3}$$

$$Standard\,deviation(stdv)=\sqrt{\frac{\sum_{i=1}^{n}(x_i-\mu)^2}{n}} \tag{3.4}$$

3.2 Stochastic Experiments

The section of the study has to do with perturbing selected Emanuel scheme control parameters by a stochastic means. Different physical processes are being parameterized for different reasons in current climate models. In the RegCM 4.7.1, all precipitation processes have been parameterized (eg. see Elguindi et al., 2006; Giorgi et al., 2016). For the West African region, precipitation is very important since most economic activities including agriculture is rain fed. It was interesting to investigate the effect of perturbing the initial conditions of one of the widely used convective scheme over the study period. Given that convective parameterization is a major source of uncertainty in model performance, it has become indispensable to represent these uncertainties in a system of n ensembles. This section attempts to quantify the uncertainty associated with the simulation of precipitation and surface temperature. It was confirmed in this section that the Emanuel scheme is not sensitive to any one of the scheme parameters (Elguindi et al., 2011; Giorgi et al., 2016). The Emanuel scheme has 14 control parameters that assume their respective "optimized" values. This study focuses on perturbing 4 key control parameters:

1. The Fraction of precipitation falling outside the cloud (σ_s)
2. The Maximum precipitation efficiency over land is ε_{max} (land)
3. The fractional area covered by unsaturated downdrafts is σ_d
4. The Auto-conversion threshold water content (elcrit)

The perturbation is done by using a random number generator that produces random numbers of uniform distribution. The choice of a "uniform distribution" is motivated by similar choice made by Emanuel (Emanuel, 1991; Emanuel & Živković-Rothman, 1999) in analyzing the mixing of cloud air and environmental air. Each perturbation is completely independent from each other but strongly correlated. Each set of perturbation is called "mix1, mix2, etc" corresponding to the parameters that are perturbed.

3.3 Simulations and Validation Datasets

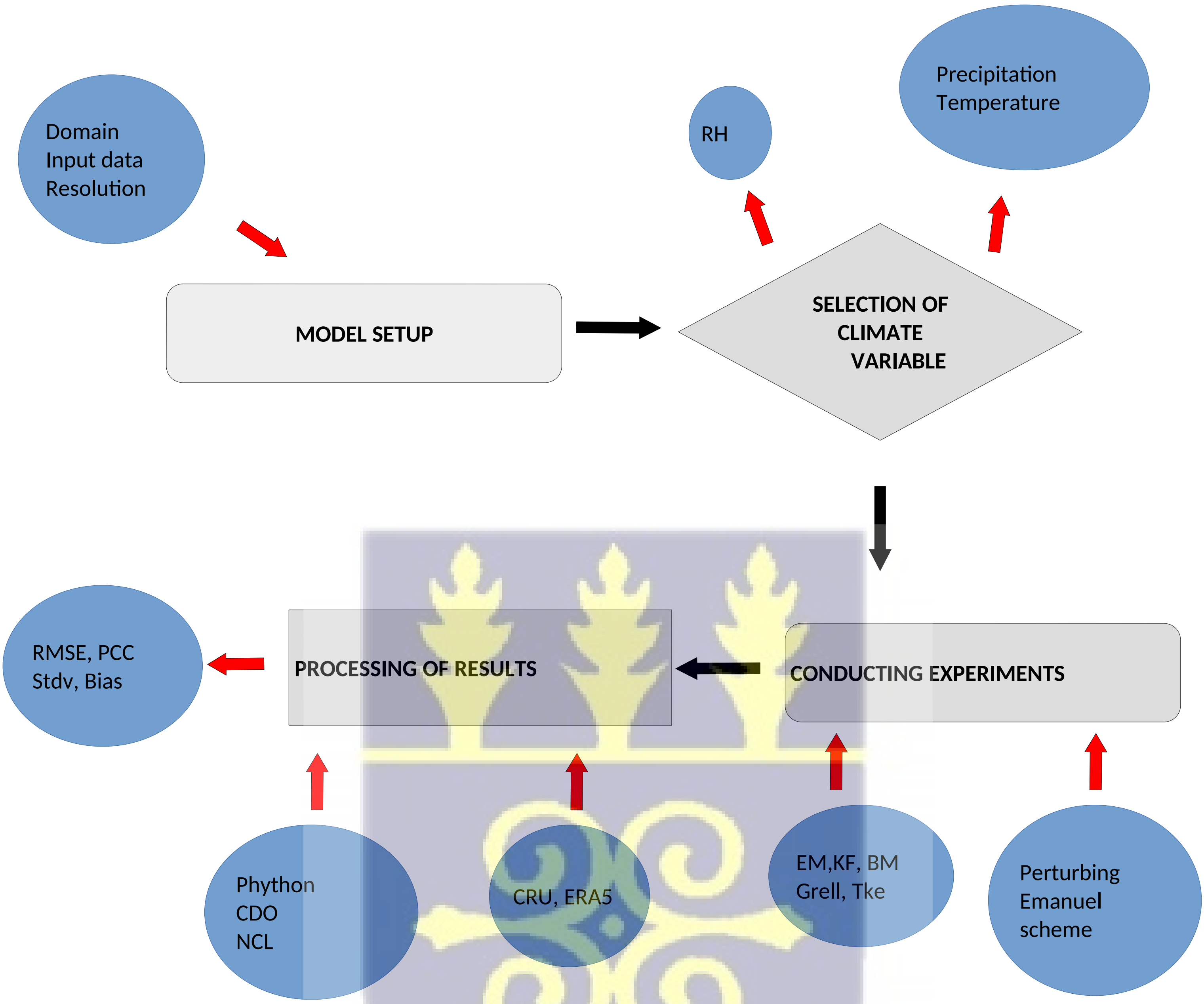

Figure 3.1: The flowchart of the methodology describing the design and implementation of numerical experiments and analyzing the results.

Due to disruption in computing resources, there have been an ensemble consisting of four members as described in Table 3.2:

Table 3.2: Descriptions of a four member ensemble formed based on the perturbation of selected Emanuel (1991) scheme control parameters

Perturbations	Parameter(s)	Description
Mix1	σ_s and σ_d were perturbed	σ_s = 0.76 - 0.99 and σ_d = 0.0001 -- 0.25
Mix2	σ_s , σ_d and ε_{max} were perturbed	σ_s = 0.76 -- 0.99 , σ_d = 0.0001 – 0.25 and ε_{max} = 0.994 – 0.999
Mix3	σ_s and σ_d were perturbed	σ_s = 0.001 -- 0.25 and σ_d = 0.001 -- 0.25
Mix4	σ_s , σ_d and ε_{max} were perturbed	σ_s = 0.001 -- 0.25 , σ_d = 0.001 -- 0.25 and ε_{max} = 0.994 – 0.999

Each “Mix” – Mix1, Mix2, Mix3 and Mix4 – is distinct by the thresholds employed in perturbing the stochastic scheme-control-parameters. All four (4) parameters perturbed are bounded by minimum (V_{min}) and maximum (V_{max}) taken from refined literature including Emanuel, (1991, 1997); Emanuel & Živković-Rothman, (1999); Grandpeix et al., (2004); Villalba-Pradas & Tapiador, (2022) in other to avoid unrealistic values. Much attention was paid to how “ε_{max}” influenced the model output particularly because Grandpeix et al., (2004) found “0.995” to be more efficient than "0.999" used by Emanuel, (1991); Emanuel & Živković-Rothman, (1999) and the RegCM infrastructure. Table 3.3 summarizes the maximum and minimum values each scheme-control-parameter can assume in the stochastic perturbation:

Table 3.3: A description of the minimum and maximum values that each control parameter can assume.

Parameter	V_{min}	V_{max}	"Optimized value"
σ_s	0	1	0.12
σ_d	0	1	0.05
ε_{max} (land)	0	1	0.99
el_{crit} (land and ocean)	0	0	1.1 (g/kg)

Depending on the physical structure of the assumed atmospheric dynamics, each parameter assumes a suitable range of values within the confines of the boundaries specified above and the new parameter value is calculated as:

$$param = V_{min} + RND * (V_{max} - V_{min}) \tag{3.5}$$

The main reason to perturb these scheme parameters stochastically is to quantify the convective parameterization uncertainty rather than just improving ensemble spread (Griffin et al., 2020; Thompson et al., 2021) even though the latter is also immensely desired. It is therefore essential to verify and be certain that these perturbations do not degrade the quality of the parameterization.

Table 3.4: General design of the RegCM 4.7.1 simulations over West Africa.

Parameters	Description
Spatial resolution	25 km
Temporal resolution	50s
Vertical levels (top)	23 layers (100 hPa)
Projection	Normal Mercator (NORMER)
Global analysis dataset	ERA-Interim (EIN15)
Boundary layer scheme	Holtslag PBL
Microphysics scheme	SUBEX (Pal et al. 2000)
Land Surface Scheme	CLM 4.5 (Steiner et al. 2009)

Precipitation and surface temperature was validated against CRU TS4 (Climatic Research Unit gridded Time Series) data that spans from 1901 to 2020 (more than 11 decades). CRU TS4 is widely used over the African region with spatial resolution of 0.5° × 0.5°. The dataset covers all terrestrial domains of the world except Antarctica and contain very few missing values. CRU is derived by interpolating monthly climate anomalies from extensive networks of weather station observations. It is updated periodically (every year) since its emergence to span more years and locations by the inclusion of additional observations from meteorological station. The interpolation process over the years has been changed with the emergence of more effective processes. The project currently uses angular-distance weighting (ADW) interpolation process. This implementation of ADW provides improved traceability between each gridded value and the input observations. CRU TS is now entirely available in FORTRAN to improve speed and portability.

CRU TS makes several variables available: Temperature (TMP), Precipitation (PRE), Diurnal Temperature Range (DTR) and Vapour Pressure (VAP) but this study uses only temperature and precipitation in NetCDF format. Each of these variables come with an embedded data on the meteorological stations that were utilized in compiling and synthesizing climate variables. The current features and interpolation methods are reported by Harris et al., (2020).

ERA5 is a fifth generation ECMWF atmospheric reanalysis climate dataset that spans January 1950 to 2021 and can be obtain as a global dataset or as a location specific dataset. The dataset is produced by Copernicus Climate Change Services at the ECMWF. A wide range of climate variables are available over both land and ocean and in each case, datasets are available on several levels (pressure, vorticity, potential temperature): these variables include but not limited to Surface Temperature, Relative humidity, Precipitation. ERA5 provides hourly, daily, and monthly estimates for these climate variables at a spatial resolution of 30 km. The atmosphere is commonly resolved into 137 levels spanning the atmosphere from the surface to approximately 80 km. In addition, each variable comes with information about possible sources of uncertainties and this makes it easier to access these uncertainties. ERA5 is not entirely an observational dataset but it combines large historical observations with highly refined modeling and some of the best data assimilation systems are used in the production.

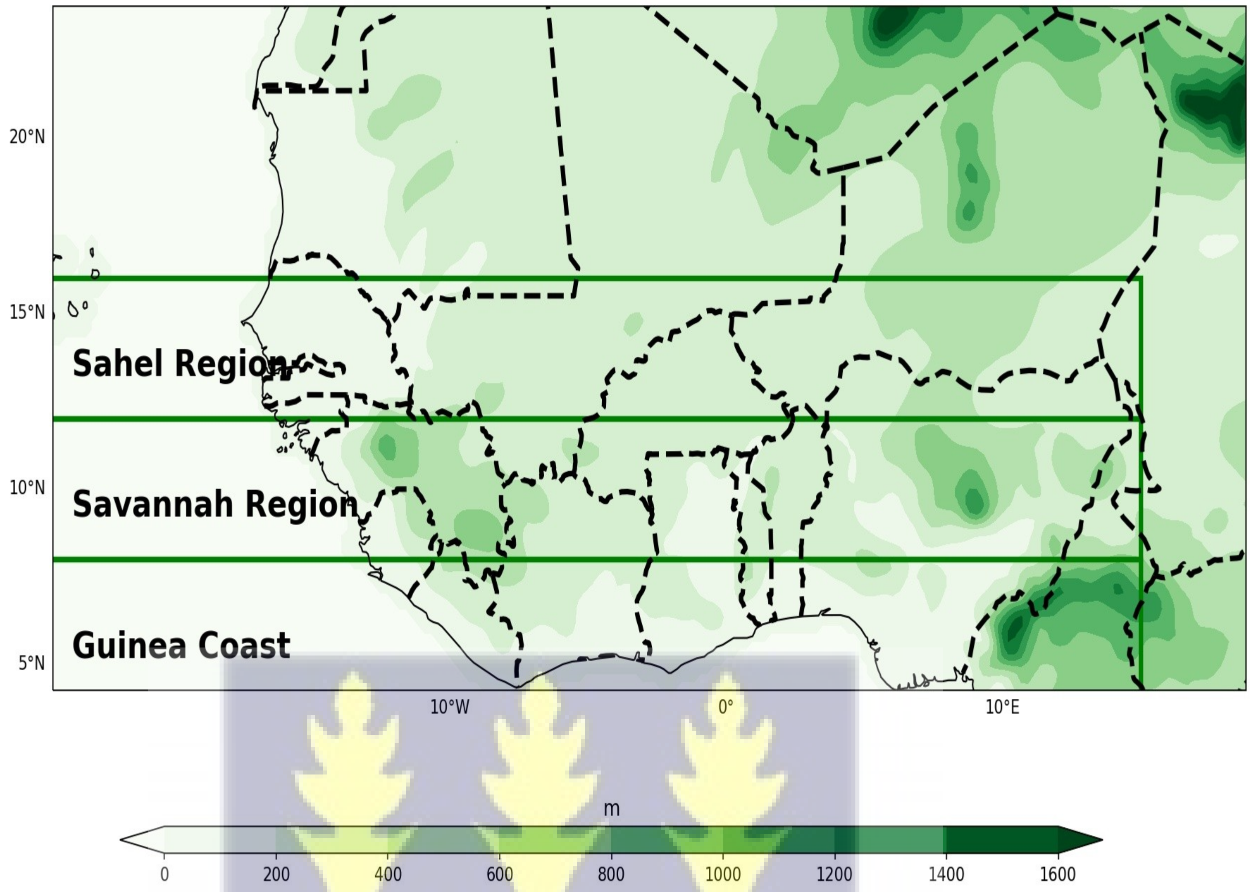

Figure 3.2: The topography (meters) of the West African region showing the three main climatic zones (Sawadogo 2019)

CHAPTER FOUR

4.0 Results and Discussions

Introduction

Under this section, the performance of the RegCM4 over the West African domain and its three main climatic zones: the Guinea Coast (GC), the Savannah Region (Sav), the Sahel Region (Sah) are presented and discussed.

4.1 WEST AFRICAN REGION

Annual temporal plots give first hand information about the model performance over the domain of interest. It is now evident more than ever that the climate is changing perhaps more rigorously than imagined owing almost entirely to global warming. The seemingly increasing intensity of global warming has significant effects on major climatic drivers such as cloud dynamics and the earth's energy budget on the region's climate pattern. This makes it intuitive to believe for a fact that annual cycles of climate may not be what the region is accustomed to hence the annual assessment of model data as they compare with well evaluated observational data is essential (Ogwang et al., 2016). The analysis was done through the 5 years average for DJF, MAM, JJA, SON and annually in each climatic zone.

4.1.1 Precipitation

The climatology of the annual cycle of precipitation averaged over the five (5) years period (2010 – 2014) of this research over the West African region is presented in Figure 4.1. Figure 4.1 reveals that higher amounts of precipitation occur from May through to October with peak values occurring around August for CRU observational data (see also Figure 4.16). The performance of each convective scheme compared to CRU is good except for Grell which appears to have significantly overestimated precipitation (see Figure 4.16), but BM and Emanuel outperformed as they align almost perfectly with the observational data with an overestimation and underestimation by

Emanuel and BM respectively. BM and Emanuel both overestimates but to a lesser extent from late January through to June and again from October to late November. The performance of KF, Tiedtke and Grell is characterized by an overestimation throughout the annual cycle (Figure 4.1).

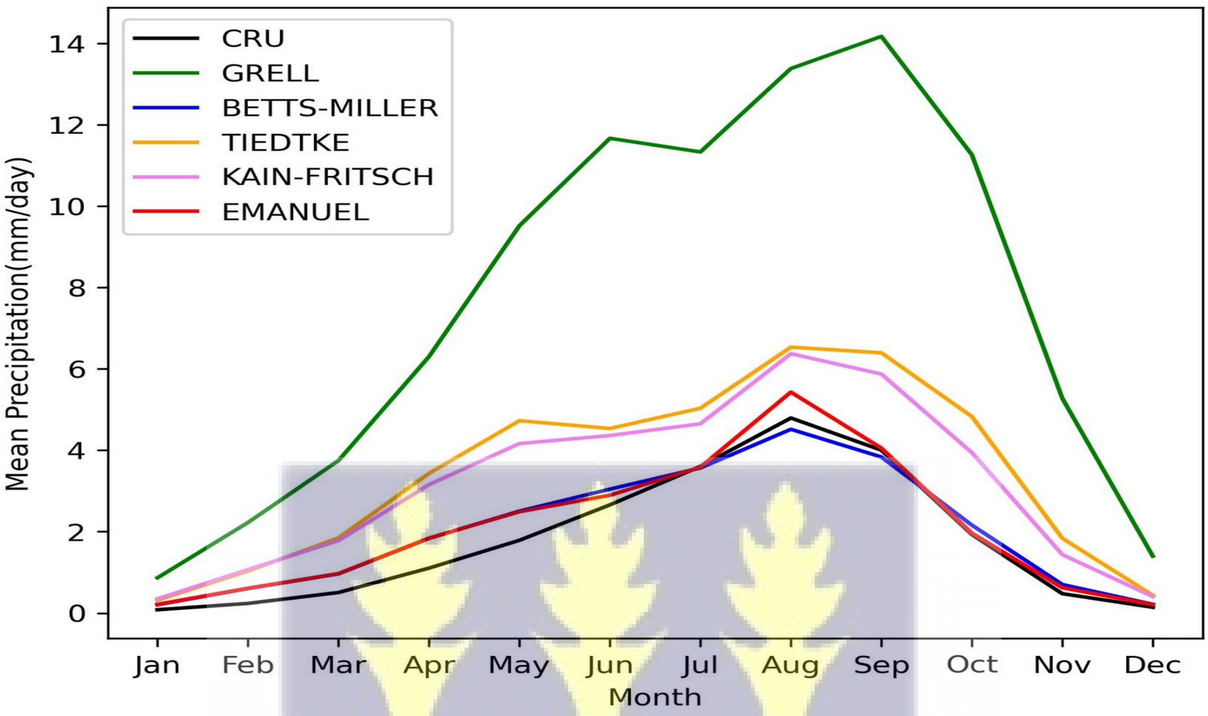

Figure 4.1: Mean Surface Temperature (°C) of Convective Schemes over West Africa in comparison with CRU observational data.

The least precipitation however occurs in the later end of November through to February. There is a generally good capture of the annual cycle of the observational datasets (CRU) by the various convective schemes with some overestimation and underestimation, the Grell scheme however showed significant overestimation compared to the others. Figure 4.2 shows the spatial mean bias of precipitation over the five (5) study years (2010 – 2014) in comparison with CRU observation dataset and indicates the performance of the five (5) convective schemes (Emanuel, Grell, KF, BM and Tiedtke) used in this study. Low mean bias values were registered in the Savannah and Sahel regions compared to the Guinea coast especially around high lands and complex topography. This is similar to the results of Adeniyi, (2014) and Kouassi et al., (2022). There has been high precipitation in the Guinea Coast as opposed to other climatic zones. This observation is consistent with observations from other studies (Adeniyi, 2014; Kouassi et al., 2022). Grell, Tiedtke and Kain-Fritsch show a high mean bias (overestimation) around 10° N towards the East and along the Guinean highlands. This is due to the usual difficulty in simulating precipitation along complex topography such as the Jos Plateau, Cameroon mountains and Guinea highlands.

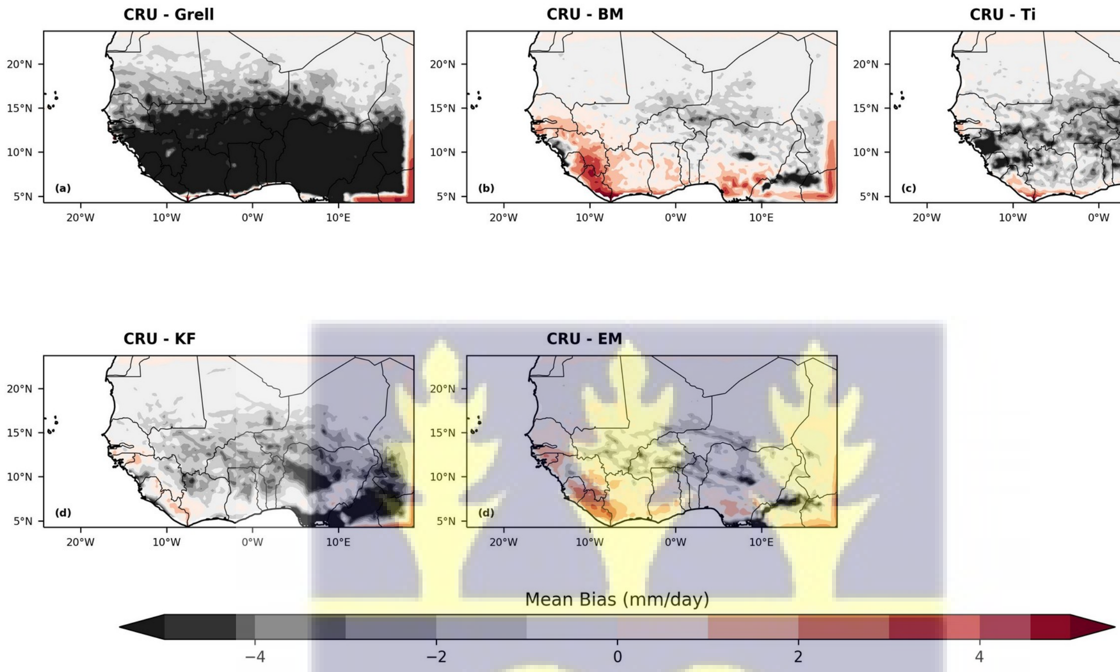

Figure 4.2: Distribution of spatial mean bias (mm/day) indicating the performance of Convective Schemes over West Africa in comparison with CRU observational data.

Even though precipitation over the West Africa region is greatly influenced by the Atlantic Ocean, it is the Guinean coast that is affected most. Mountainous areas are also known to experience heavy rainfalls due to forced convection over these areas. South westerly winds from the Atlantic Ocean are forced up by the mountains hence causing condensation and leading to the formation of precipitation (Adeniyi, 2014). It is interesting to see the convective scheme capturing these dynamics to varying degrees. Emanuel produces fairly low bias values even over this complex topographic regions and this is interesting and contradicts the report by Adeniyi, (2014). Such accuracy maybe attributed to the more realistic and practical theory the Emanuel scheme is based on: several observational evidence have supported that rather than a continuous mixing, the buoyancy sorting method is more realistic. The buoyancy sorting method assumes mixing of cloudy air and environmental air to be highly episodic and inhomogeneous. Air from the environment entrains into a cloud and mixes with the cloud in different fractions (inhomogeneous) hence the different fractions of mixtures will have different buoyancies due to different densities and temperatures (Emanuel, 1991). BM, Grell, Tiedtke and KF capture the dynamics over these complex terrains well but tails Emanuel in this regard. The bias of the the various convective schemes with regard to the CRU observational datasets in the West African region is further presented in Table 4.1. Table 4.1 shows the mean bias for DJF, MAM, JJA, SON and annually. The values show major overestimation by Grell across all study periods with a maximum of 6.99 mm/day occurring in the months of JJA. The varying degree of overestimation seen in all schemes can be attributed to the manner of implementation of the quasi-equilibrium assumption. This assumption states that the convective activity of clouds removes atmospheric instability introduced by large-scale processes. There is a good chance that this assumption becomes over-active over the tropics since convective is widely known to be vigorous.

Table 4.1: Mean bias (MB) for the average precipitation (2010 - 2014) for model simulations in comparison with CRU observational datasets.

Scheme	DJF	MAM	JJA	SON	Annual
Grell	-1.05	-4.28	-6.99	-6.49	-4.7
BM	-0.17	-0.66	-0.59	-0.41	-0.46
Tiedtke	-0.36	-1.85	-1.86	-2.02	-1.52
KF	-0.37	-1.62	-1.67	-1.56	-1.31
Emanuel	-0.17	-0.66	-0.79	-0.39	-0.5

This has been seen to be very profound in Grell (Adeniyi, 2014). This pattern of peaking bias in the month of JJA was seen in all schemes except BM and Tiedtke which peaked in MAM and SON respectively (see Table 4.1). Judging by the statistical metrics used in this study (see Table 4.1 and Table 4.2), BM and Emanuel performs better in comparison with CRU observational data with maximum mean bias of 0.66 mm/day and 0.79 mm/day respectively. This was evident also in comparison of the computed values for the RMSE for these two schemes (see Table 4.2). Emanuel and BM performed relatively better with intermittent performance from KF. In each of these months, Emanuel has maintained a good performance illustrated by a relatively low RMSE and high PCC. The lowest RMSE value of 0.51 mm/day was computed for Emanuel in DJF.

Table 4.2: RMSE and PCC for the average precipitation (2010 - 2014) for model simulations in comparison with CRU observational datasets.

Scheme	DJF		MAM		JJA		SON		Annual	
	RMSE	PCC	RMSE	PCC	RMSE	PCC	RMSE	PCC	RMSE	PCC
Grell	3.73	0.57	10.69	0.51	13.12	0.61	14.43	0.65	11.27	0.62
BM	0.56	0.63	1.79	0.59	3.54	0.54	2.64	0.63	2.40	0.62
Tiedtke	1.32	0.56	5.35	0.46	4.91	0.55	5.49	0.61	4.60	0.56
KF	1.14	0.66	3.53	0.61	4.30	0.61	3.77	0.7	3.41	0.66
Emanuel	0.51	0.73	1.61	0.7	3.26	0.66	2.16	0.74	2.13	0.72

The months MAM and JJA are very important in West Africa as they mostly define the wet months. Emanuel again produces the lowest RMSE values of 1.61 mm/day, and 3.26 mm/day respectively with very good correlations. Grell on the other hand has been consistent in overestimating precipitation over the West African region by the largest margin relative to Emanuel, BM, Tiedtke and KF. It produced the highest RMSE value of 14.43 mm/day in the months of SON while producing its lowest RMSE value of 3.73 mm/day in the months of DJF. All schemes correlates well with the worst correlation value of 0.46 produced by Tiedtke in the months of MAM. Emanuel can be taken as the most appropriate scheme over West Africa as it has low RMSE and relatively good PCC. The correlations produced by KF is worth looking at as they fall short only relative to those of Emanuel. Wet bias is the dominant feature seen over West Africa across all schemes and all study periods.

4.1.2 Temperature

Figure 4.3 shows the annual climatology of surface temperature averaged over the the study period (2010 – 2014) over the West African region. Figure 4.3 reveals the general performance of the five convective schemes and the observational CRU dataset. It is again evident that the various convective schemes captures realistically the mean 2m-temperature (surface) over the West African region. There is a general warm bias of all the convective schemes in January through to May where the first peaking occurs (~ 32.5 °C). From this perspective, Grell seems to have outperformed KF, Emanuel, Tiedtke and BM. The second relatively lower peak (~30 °C) is seen to occur around September, October months. Between November and December, a steep decline is seen for Emanuel, BM and Grell. Figure 4.4 on the other hand shows the spatial performance of the five convective schemes in comparison with CRU surface temperature. Mean temperature ranges from 19 °C to 30 °C within the five years period (2010 – 2014). All schemes show similar spatial distribution of surface temperature with varying degree of overestimation and underestimation in relation to the observational dataset (CRU). There was no clear observation of the meridional surface temperature gradient zone between the Guinea coast and the Savannah region. This is due to the fact that this is an averaged over the entire year over which the characteristics of the zone changes. The simulation of the meridional surface temperature gradient zone is clear in the spatial plots for the individual months (DJF, MAM, JJA and SON. See Figure 4.18). The schemes used in this study did a better job simulating surface temperature over complex terrains than they did simulating precipitation. This is important since such complexities are main drivers on local climate in the study area (Koné et al., 2018). High temperatures were observed in the northern part of the Savannah region through the Sahel region. None of the schemes depicted "evaporated cooling" as a results of overestimation of precipitation. This characteristic is expected to be exhibited in the sub-regions of the West African domain, and adds to a list of reasons why sub-domain analysis in sensitivity tests are important. Tiedtke and BM greatly overestimation surface temperature (see Table 4.3) as compared to other schemes. Grell and Emanuel overestimate but are relatively mild as shown in Table 4.3. It is hence not surprising to see a good spatial distribution of surface temperature produced by Emanuel (Figure 4.4). This was well captured in the RMSE values computed for the various schemes. The values for Emanuel, Grell and KF were outstanding throughout the months of DJF, MAM, JJA, SON and annually as shown in Table 4.4. Emanuel produced low surface temperature values between 5° and 10° N compared to the results from other schemes. This may probably be due to the transportation of heat by an unsaturated downdraft and the dependence of auto-conversion threshold water content on temperature (Emanuel & Živković-Rothman, 1999). There is not much difference between the PCC in each month of analysis but all correlations were good, mostly towering above 0.6 with Emanuel correlating well consistently. All schemes produced a warm bias but to a varying degree. Grell, Emanuel, and KF have been consistent in producing lower RMSE values with high correlations.

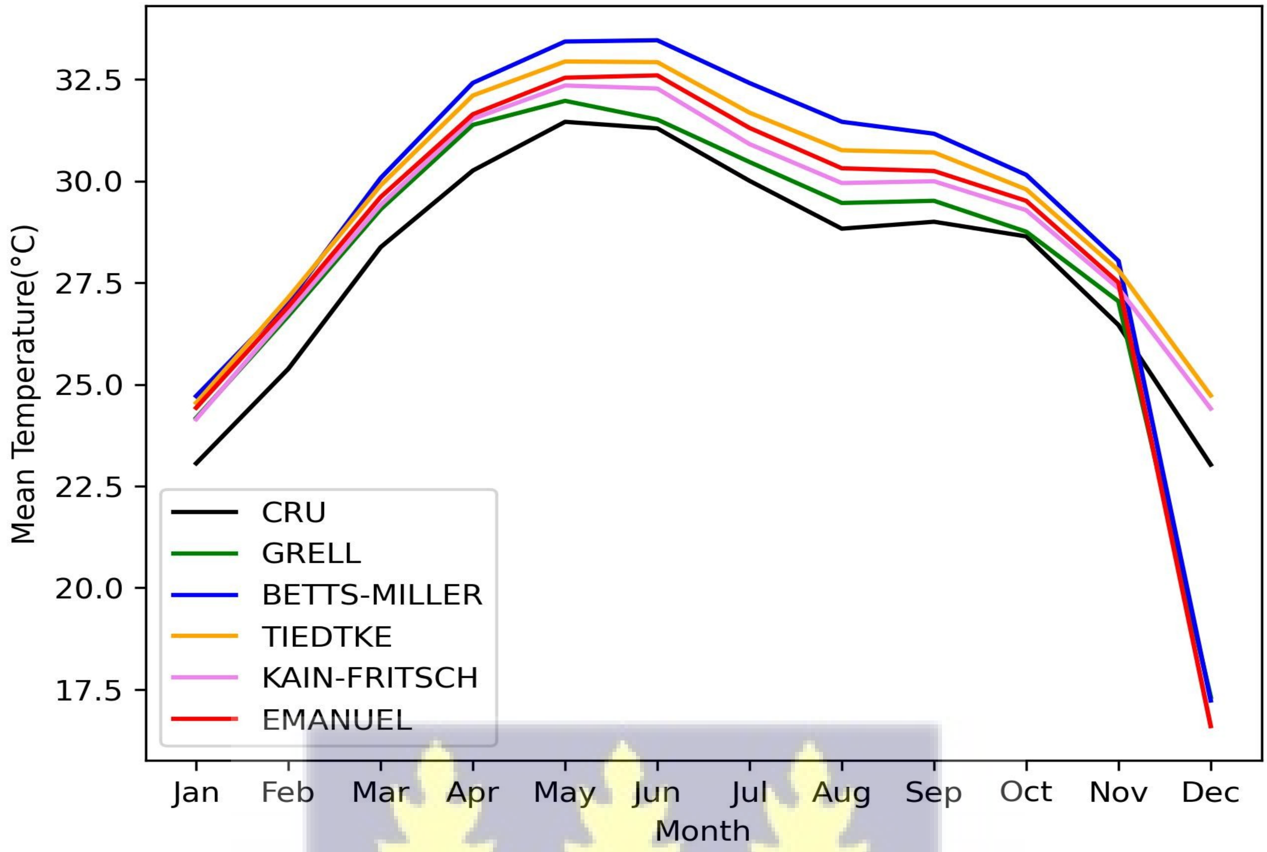

Figure 4.3: Mean Surface Temperature (°C) of Schemes over West Africa in comparison with CRU observational data.

Table 4.3: Mean bias (MB) for the mean temperature (2010 - 2014) for model simulations in comparison with CRU observational datasets

Scheme	DJF	MAM	JJA	SON	Annual
Grell	-3.02	-5.47	-5.16	-4.82	-4.62
BM	-3.22	-6.30	-6.65	-5.84	-5.50
Tiedtke	-5.10	-6.05	-6.15	-5.58	-5.72
KF	-4.82	-5.63	-5.59	-5.15	-5.30
Emanuel	-2.95	-5.76	-5.86	-5.31	-4.97

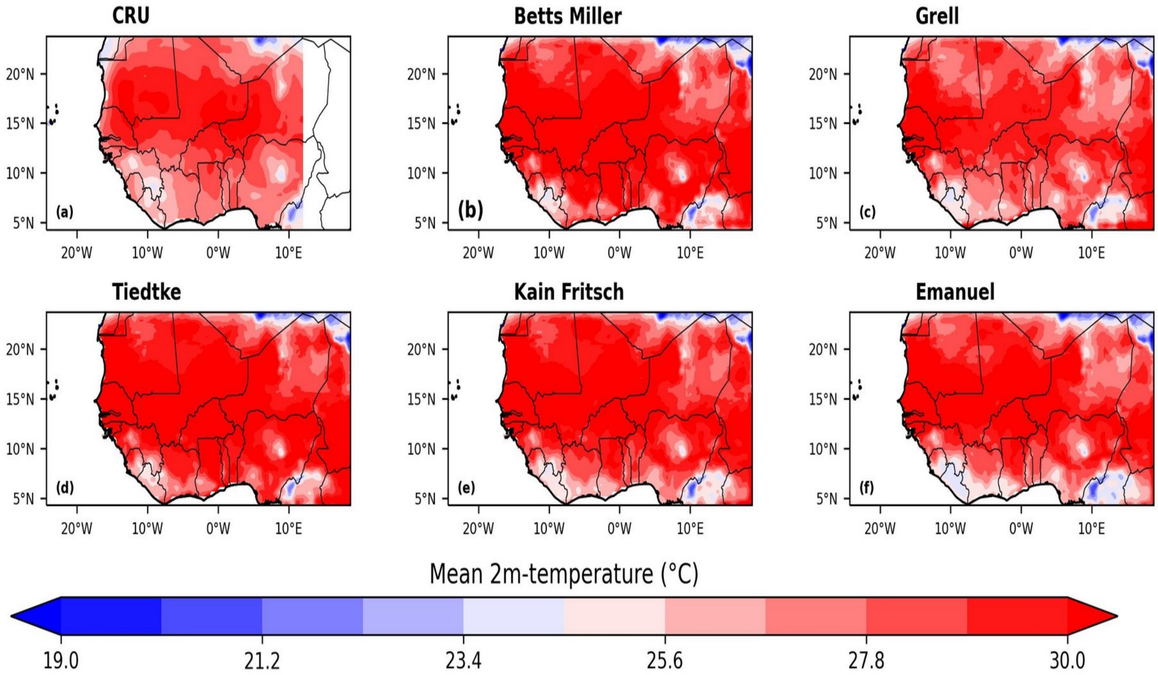

Figure 4.4: Spatial distribution of mean surface temperature (°C) of Schemes over West Africa in comparison with CRU observational data.

Table 4.4: RMSE and PCC for the mean surface temperature (2010 - 2014) for model simulations in comparison with CRU observational datasets.

Scheme	DJF		MAM		JJA		SON		Annual	
	RMSE	PCC	RMSE	PCC	RMSE	PCC	RMSE	PCC	RMSE	PCC
Grell	10.16	0.66	12.67	0.68	12.85	0.66	11.9	0.66	11.94	0.67
BM	10.3	0.66	13.01	0.69	13.36	0.69	12.16	0.69	12.26	0.69
Tiedtke	10.87	0.68	13.02	0.68	13.15	0.68	12.13	0.68	12.33	0.69
KF	10.63	0.68	12.65	0.69	12.73	0.69	11.77	0.69	11.98	0.69
Emanuel	10.2	0.66	12.67	0.69	12.8	0.7	11.75	0.7	11.9	0.69

4.1.3 Relative Humidity

Figure 4.5 shows the annual climatology of relative humidity averaged over the the study period (2010 – 2014) over the West African region. It is also a revelation of the performance of the convective schemes in simulating West African relative humidity profiles as compared to ERA5 reanalysis dataset. The model level, kz = 0.87 was chosen for analysis. The performance of all schemes are substantial compared to the reanalysis data.

Table 4.5: Mean bias (MB) for the mean relative humidity (2010 - 2014) for model (kz = 0.87) simulations in comparison with ERA5 dataset.

Scheme	DJF	MAM	JJA	SON	Annual
Grell	-4.96	-7.66	-10.77	-7.56	-7.74
BM	-3.85	-6.22	-6.21	-5.68	-5.49
Tiedtke	-5.82	-9.38	-11.25	-9.35	-8.95
KF	-2.37	-10.12	-11.22	-9.61	-8.33
Emanuel	-3.88	-8.62	-8.40	-7.28	-7.05

The months of DJF experienced the lowest values of relative humidity whiles a peak value of more than 60% was observed around August. This coincides well with the precipitation profiles discussed in subsection 4.1.1. The spatial plots of relative humidity as shown in shown in Figure 4.5 and Figure 4.6 exhibits high correlations over both land and ocean. It is therefore intuitive to predict high correlation values for relative humidity. It is also evident that northern Savannah and Sahel regions experience relatively low values of RMSE and Bias which translates in low precipitation mentioned earlier in subsection 4.1.1. As was expected from the model's performance in simulating precipitation, the schemes have overestimated relative humidity significantly as illustrated by the values of mean bias calculated (Table 4.5) for each convective scheme. The error between model simulation and ERA5 is captured by the RMSE column of Table 4.6. BM and Emanuel have consistently performed better relative to the other convective schemes (see Table 4.5 and 4.6). This is quite impressive for Emanuel to outperform the Grell convective scheme in simulating relative humidity; The Grell scheme regulates the degree of moistening and heating with the cooling impact during downdrafts due to detrainment and mass fluxes at the top and bottom of the cloud and this makes it very good for simulating relative humidity over the tropics (Elguindi et al., 2006, 2011; Giorgi et al., 2016). The PCC computed vary only minutely and the values for the RMSE are relatively large, this is due to the hurdling difficulty in simulating atmospheric humidity; accounting for atmospheric humidity is literally an atmospheric micro-physics problem, which means schemes would have to dedicate several pages for the inclusion of micro-physical dynamics in the construction of convective schemes and this by far is one of the stalling problems confronting the community (Emanuel, 1997; Emanuel & Živković-Rothman, 1999).

Table 4.6: RMSE and PCC for the mean relative humidity (2010 - 2014) for model simulations (kz=0.87) in comparison with ERA5 dataset.

Scheme	DJF		MAM		JJA		SON		Annual	
	RMSE	PCC	RMSE	PCC	RMSE	PCC	RMSE	PCC	RMSE	PCC
Grell	11.41	0.87	18.26	0.81	24.05	0.77	19.46	0.81	18.85	0.82
BM	10.71	0.87	16.88	0.82	23.27	0.75	18.85	0.81	18.00	0.82
Tiedtke	11.41	0.88	18.36	0.83	24.80	0.76	20.02	0.82	19.25	0.83
KF	11.44	0.84	19.51	0.80	25.23	0.74	20.35	0.81	19.76	0.81
Emanuel	10.72	0.87	17.67	0.83	23.92	0.75	19.56	0.80	18.59	0.82

The competing PCC values does not come as a surprise as it was expected from Figure 4.6.

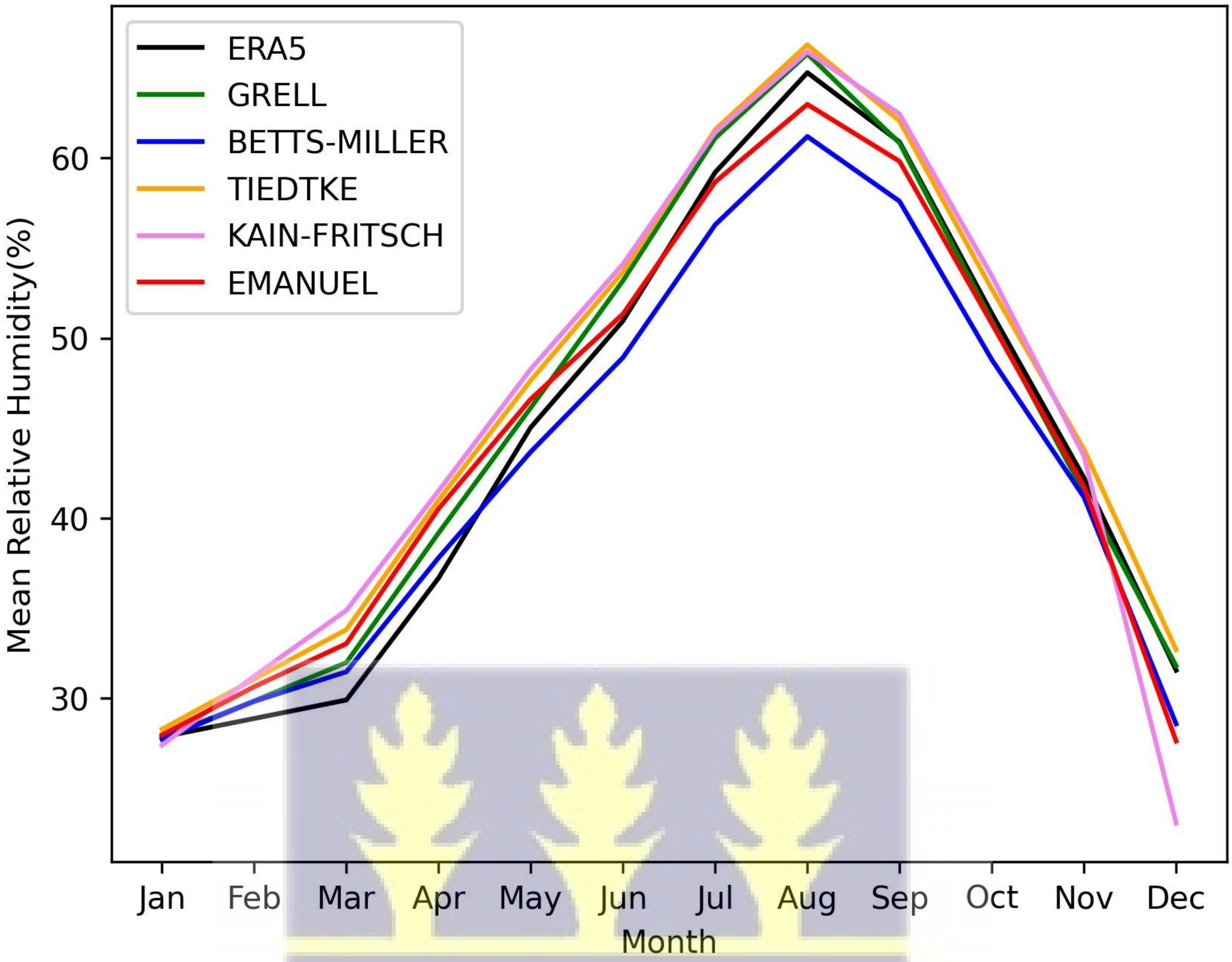

Figure 4.5: Mean relative humidity (%) of Schemes over West Africa in comparison with ERA5 reanalysis data.

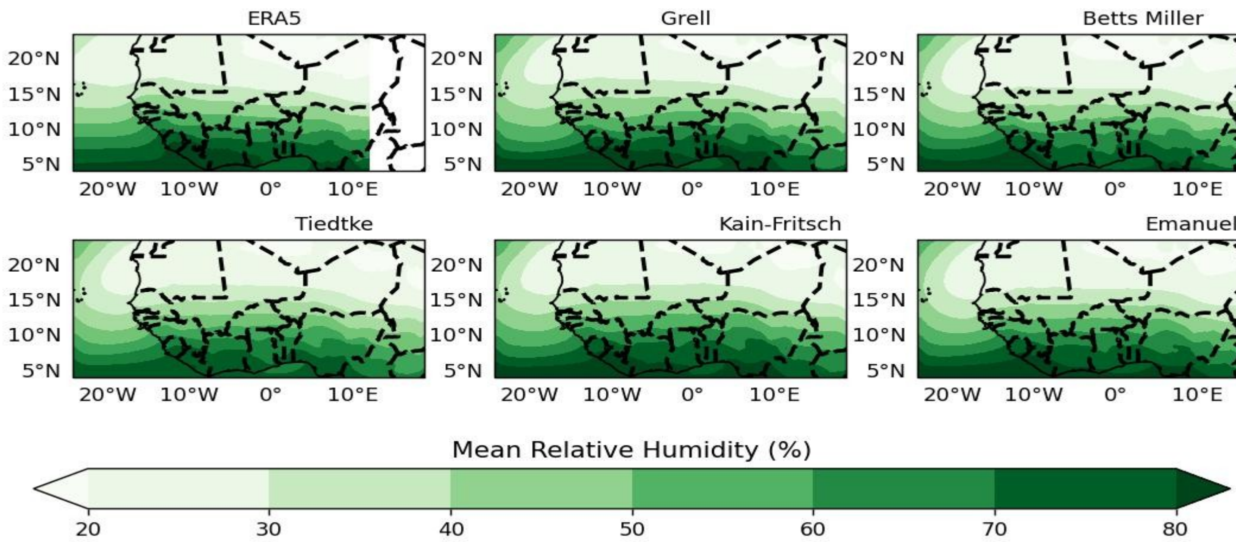

Figure 4.6: Spatial distribution of mean relative humidity (%) of Schemes over West Africa in comparison with ERA5 observational data.

4.2 Guinea Coast

4.2.1 Precipitation

Just as was seen and discussed over the entire West African domain, the results for each climatic zone is now displayed and converging and diverging points in the performance of the five convective schemes in simulating the profiles of the variables considered in this study is discussed. Beginning with the annual cycle of precipitation averaged over the Guinea Coast for the study period (2010 – 2014) is shown in Figure 4.7. A behavior as seen in Figure 4.7 is not very far from what was observed in Figure 4.1 but for a slight dynamics of BM between the months of May and October. Grell still significantly overestimated and BM and Emanuel outperformed other schemes

Table 4.7: Mean bias (MB) for precipitation (2010 - 2014) for convective schemes in comparison with CRU dataset.

Scheme	DJF	MAM	JJA	SON	Annual
Grell	-1.59	-4.18	-7.81	-9.66	-5.81
BM	-0.13	-0.14	1.16	0.54	0.36
Tiedtke	-0.48	-1.01	-1.30	-2.46	-1.31
KF	-0.36	-1.03	-0.62	-1.76	-0.94
Emanuel	-0.13	-0.28	0.16	0.17	-0.02

in the region. Emanuel is the closest in performance to the CRU observational data but unlike Figure 4.1, BM lies lower than the observational data hence attains a peak value that is significantly lower than observed in Figure 4.1. The performance of KF and Tiedtke is as observed in Figure 4.1. There is again a general good capture of the annual cycle of precipitation by the various convective schemes with some overestimation and underestimation in this region as well. Table 4.7 shows the mean bias for DJF, MAM, JJA, SON and annually computed with respect to CRU observational dataset. The values show minor overestimation by all the schemes except for BM and Emanuel in the months of JJA and SON. Grell still performs worst as compared the other schemes as per the statistical metrics employed here as shown in both Table 4.7 and Table 4.8. It is also clear the dynamics shown in the metrics calculated for the various group of months and annually.

Table 4.8: RMSE and PCC for the mean precipitation (2010 - 2014) for the five (5) convective schemes in comparison with CRU dataset.

Scheme	DJF		MAM		JJA		SON		Annual	
	RMSE	PCC	RMSE	PCC	RMSE	PCC	RMSE	PCC	RMSE	PCC
Grell	4.98	0.69	9.36	0.78	11.04	0.76	16.45	0.73	11.23	0.75
BM	0.48	0.78	1.34	0.79	3.59	0.59	2.53	0.79	2.31	0.76
Tiedtke	1.40	0.70	2.25	0.80	3.79	0.71	5.17	0.69	3.47	0.75
KF	0.79	0.82	1.99	0.78	2.91	0.77	3.46	0.79	2.50	0.81
Emanuel	0.43	0.84	1.27	0.83	2.61	0.79	2.12	0.84	1.81	0.85

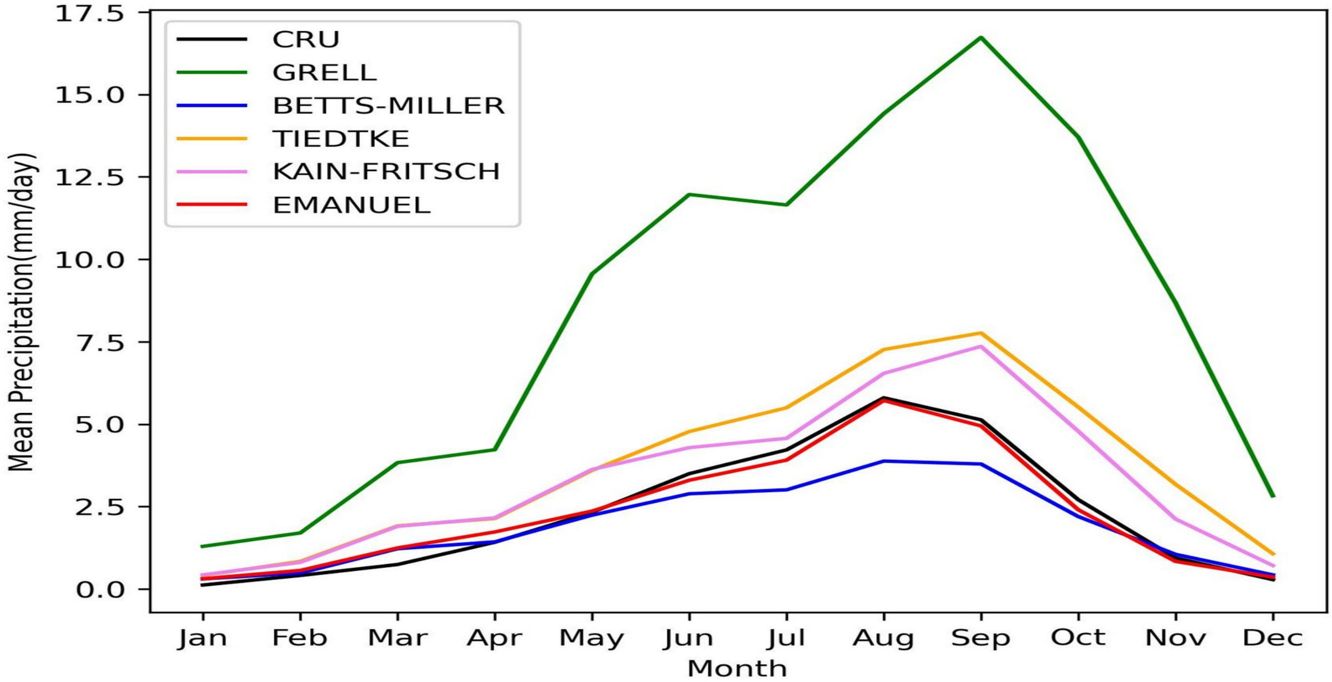

Figure 4.7: Mean precipitation (mm/day) of Schemes over Guinea Coast in comparison with CRU observational data

4.2.2 Surface Temperature

Figure 4.8 shows the annual climatology of surface temperature averaged over the the study period (2010 – 2014) over the Guinean Coast just as was seen in Figure 4.3. The dynamics of precipitation seen and discussed in Figure 4.3 is not very different from that of Figure 4.8 except for some change in the performance of Grell around the month of May. The spatial performance of the Guinean Coast is same as represented in Figure 4.4. Table 4.9 represents the performance of the five (5) convective schemes in simulating surface temperature in the Guinean Coast measured by mean bias.

Table 4.9: Mean bias (MB) for surface temperature (2010 - 2014) for convective schemes in comparison with CRU dataset.

Scheme	DJF	MAM	JJA	SON	Annual
Grell	0.58	-1.51	-0.29	-0.43	-0.41
BM	0.087	-2.49	-2.60	-2.16	-1.79
Tiedtke	-2.01	-2.08	-1.77	-1.61	-1.87
KF	-1.78	-1.69	-1.29	-1.17	-1.48
Emanuel	0.46	-1.68	-1.48	-1.47	-1.04

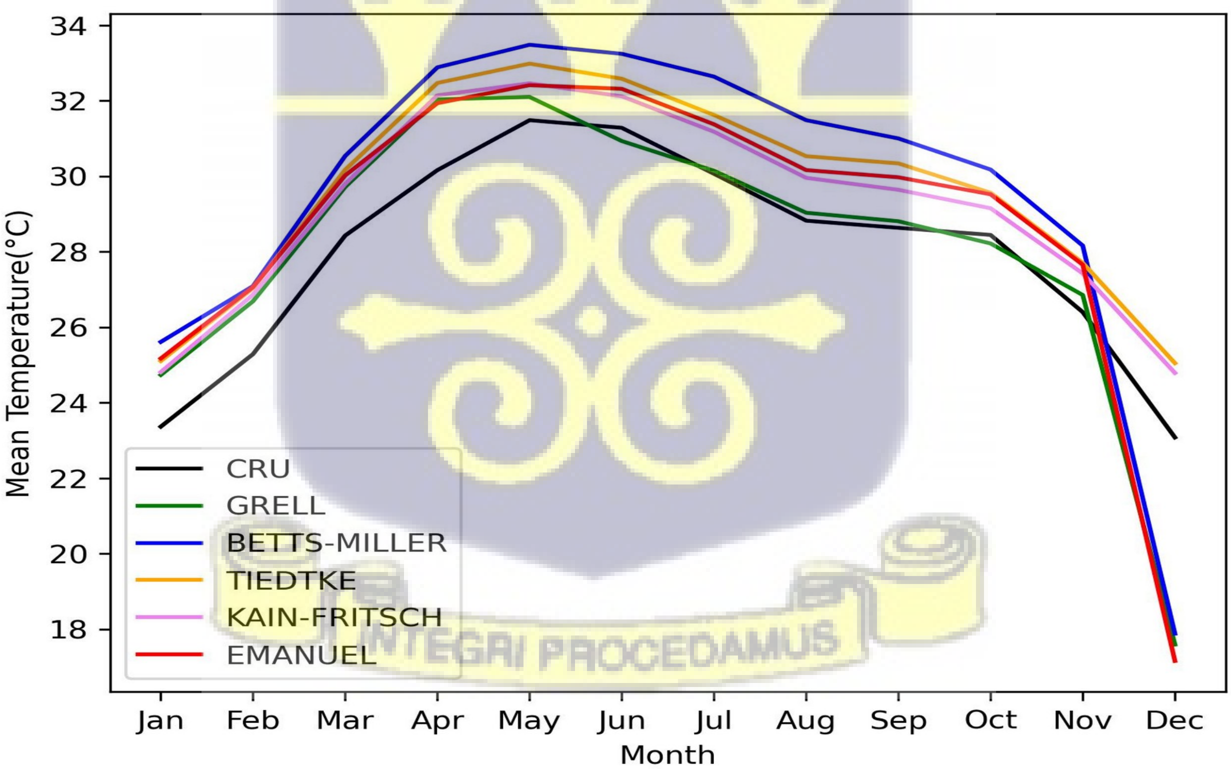

Figure 4.8: Mean surface temperature (°C) of Schemes over Guinea Coast in comparison with CRU

Table 4.10: RMSE and PCC for the surface temperature (2010 - 2014) for the five (5) convective schemes in comparison with CRU dataset.

Scheme	DJF		MAM		JJA		SON		Annual	
	RMSE	PCC	RMSE	PCC	RMSE	PCC	RMSE	PCC	RMSE	PCC
Grell	5.36	0.72	4.18	0.86	3.54	0.90	3.59	0.85	4.23	0.85
BM	5.816	0.71	4.71	0.86	4.23	0.92	4.19	0.87	4.78	0.86
Tiedtke	4.96	0.79	4.44	0.87	3.74	0.92	3.82	0.87	4.27	0.88
KF	4.75	0.79	4.12	0.88	3.55	0.92	3.61	0.88	4.04	0.88
Emanuel	5.76	0.71	4.15	0.88	3.61	0.92	3.81	0.87	4.41	0.86

A varying degree of overestimation and underestimation can been seen in Table 4.9. All schemes except Grell, BM, and Emanuel consistently showed warm bias in the coast. Grell, BM and Emanuel however showed cold bias in the months of DJF by 0.58 °C, 0.087 °C, and 0.46 °C respectively. There have been generally small deviations (overestimation or underestimation) from the observation. This also translated into the relatively better RMSE statistical metric computed and represented in Table 4.10. Table 4.10 indicates a better performance of the convective schemes as compared to the afore discussed results in Table 4.4. KF produced low RMSE values over the period of DJF, MAM and the annual analysis. Grell marginally outperforms KF and the other in JJA and SON. The correlation values again are seen to be very similar with KF marginally outperforming the rest. It is interesting to see Grell, BM and Emanuel exhibiting a cold bias in DJF in agreement with the theory that more rainfall should lead ideally to more evaporative cooling hence lower temperatures. This theory again explains that the warm bias simulated by BM and Emanuel in JJA and SON is as a result of the dry bias (see Table 4.7) observed in the same months.

4.2.3 Relative Humidity

It was noticed that all five (5) convective schemes did not do a good work simulating relative humidity in the West African region as compared to their performance in simulating precipitation and surface temperature. The striking similarity of Figure 4.9 and Figure 4.5 can not be ignored. The same dynamics is observed besides some slight deviations. Table 4.11 and 4.12 represents the mean bias, the RMSE and the PCC of model as computed in relation to ERA5 reanalysis data. A much smaller bias and error are seen here (Table 4.11 and 4.12) as compared to Table 4.5 and 4.6. This have resulted in a significant increase in the correlation recorded (see Table 4.12) as indicated by Figure 4.6. There have been varying degree of overestimation as well as underestimation by the convective schemes as shown in Table 4.11. Tiedtke overestimated relative humidity through all months, Grell overestimates in the months of DJF, and JJA. Emanuel overestimates only in MAM while KF underestimates only in DJF. Grell outperforms in the months of DJF, and annually while only tailing Tiedtke in MAM, and Emanuel in SON. The correlations of all schemes were impressive with the worst value being 0.96.

Table 4.11: Mean bias (MB) for relative humidity (2010 - 2014) for convective schemes in comparison with ERA5 dataset.

Scheme	DJF	MAM	JJA	SON	Annual
Grell	-0.19	1.11	-1.25	0.98	0.16
BM	1.07	2.28	5.34	3.58	3.07
Tiedtke	-1.72	-2.39	-2.12	-2.66	-2.22
KF	2.32	-2.42	-1.21	-1.96	-0.82
Emanuel	0.71	-1.91	1.30	0.63	0.18

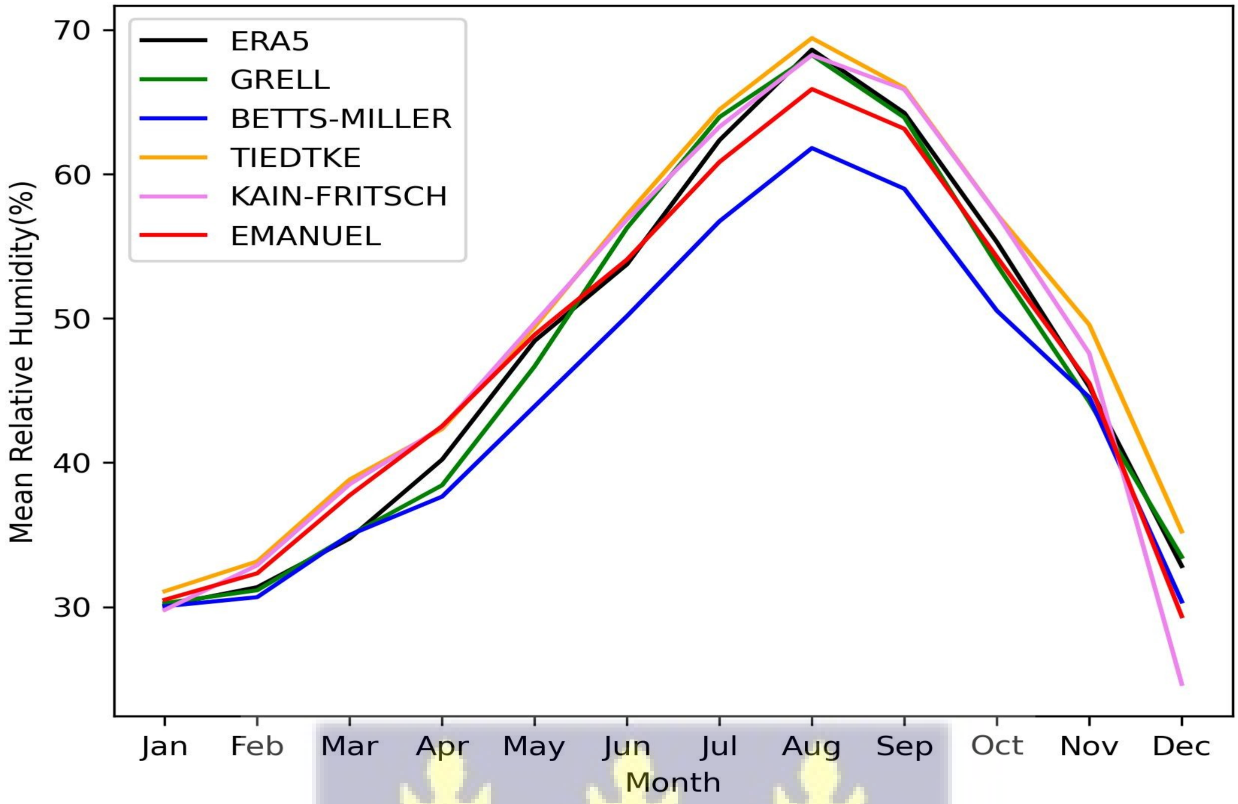

Figure 4.9: Mean relative humidity (%) of Schemes over Guinea Coast in comparison with ERA5 reanalysis data.

Table 4.12: RMSE and PCC for relative humidity (2010 - 2014) of the five (5) convective schemes in comparison with ERA5 dataset

Scheme	DJF		MAM		JJA		SON		Annual	
	RMSE	PCC	RMSE	PCC	RMSE	PCC	RMSE	PCC	RMSE	PCC
Grell	3.10	0.99	4.40	0.99	5.48	0.99	3.17	0.99	4.15	0.99
BM	3.82	0.98	5.58	0.99	7.59	0.99	5.31	0.99	5.73	0.99
Tiedtke	4.49	0.99	3.94	0.99	3.86	0.99	4.63	0.99	4.24	0.99
KF	6.43	0.96	5.00	0.99	4.28	0.99	4.00	0.99	5.01	0.99
Emanuel	4.09	0.98	5.21	0.99	4.18	0.99	3.06	0.99	4.21	0.99

4.3 Savannah Region

4.3.1 Precipitation

There has been a fall in precipitation over the Savannah region as indicated by the CRU observational dataset (see Figure 4.10) as compared to what was observed in the Guinean Coast (Figure 4.7). This is expected due to varying climatic characteristics of the these regions (Kouassi et al., 2022). Figure 4.10 suggests a better performance of the BM convective scheme. This observation is validated by values of RMSE and bias computed for all the convective schemes (see Table 4.13 and 4.14). Grell have again exhibited poor performance in simulating precipitation with consistent large RMSE values (see Table 4.14). As shown in Figure 4.10, Grell has significantly overestimated precipitation again in the Savannah region (this is confirmed by large negative bias values). BM performs outstandingly by the metrics recorded in Table 4.13 and Table 4.14.

Table 4.13: Mean bias (MB) for precipitation (2010 - 2014) for convective schemes in comparison with CRU dataset over the Savannah region.

Scheme	DJF	MAM	JJA	SON	Annual
Grell	-1.82	-4.03	-6.38	-6.80	-4.76
BM	-0.30	-0.56	-0.26	-0.26	-0.34
Tiedtke	-0.62	-1.60	-1.75	-1.81	-1.45
KF	-0.56	-1.54	-1.46	-1.49	-1.26
Emanuel	-0.30	-0.64	-0.78	-0.33	-0.51

Table 4.14: RMSE and PCC for precipitation (2010 - 2014) of the five (5) convective schemes in comparison with CRU dataset over the Savannah region.

Scheme	DJF		MAM		JJA		SON		Annual	
	RMSE	PCC	RMSE	PCC	RMSE	PCC	RMSE	PCC	RMSE	PCC
Grell	4.10	0.81	6.15	0.78	8.90	0.80	11.05	0.72	8.00	0.77
BM	0.69	0.77	1.41	0.71	2.20	0.69	1.22	0.85	1.48	0.79
Tiedtke	1.49	0.68	2.83	0.67	3.56	0.71	3.25	0.77	2.89	0.76
KF	1.09	0.81	2.34	0.74	2.76	0.80	2.59	0.81	2.29	0.82
Emanuel	0.60	0.82	1.22	0.82	2.36	0.75	1.33	0.85	1.52	0.83

BM produced the least RMSE values as well as bias. Even though it performs well, the bias indicates that the scheme overestimated through out the study period. Emanuel tails only BM in performance in terms of the metrics used in this study. The general structure of this is not so different from the dynamics shown by the convective schemes in simulating precipitation in the Guinean Coast and over West Africa.

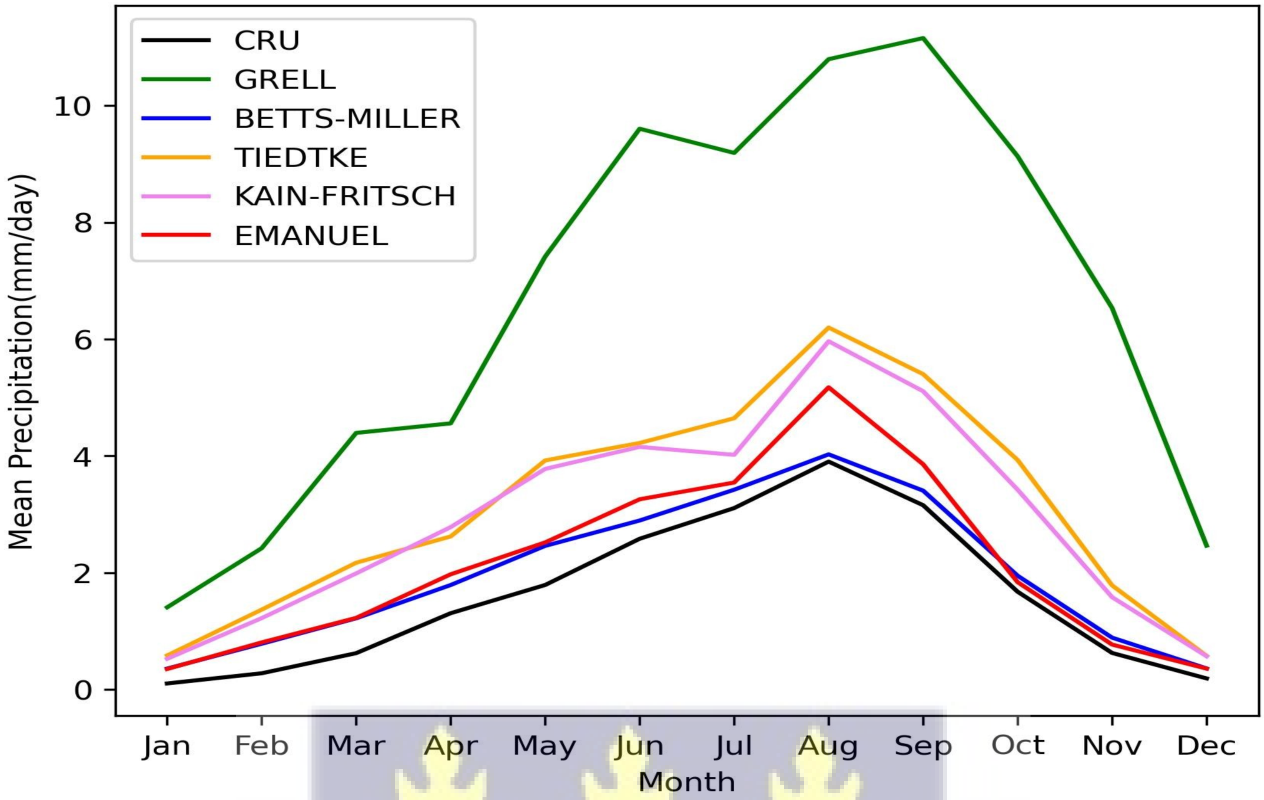

Figure 4.10: Mean precipitation (mm/day) of Schemes over Savannah region in comparison with CRU observational data.

4.3.2 Surface Temperature

The performance of the various convective schemes shown in Figure 4.11 is no different from what was observed and discussed in Figure 4.3 and 4.8. Table 4.15 and 4.16 speaks volume to performance as compared to what was discussed in the Guinean and West African region. The performance of the schemes in the Guinean Coast and in the Savannah region depicts good performance as seen in the statistical metrics as compared to that seen in the West African region. Several authors including (Koné et al., 2018) for this reason have recommended that statistical comparison be done over sub-regions. It is also worth noting the consistency in the wet bias observed in Table 4.13 for Emanuel (DJF) and the colder bias observed in Table 4.15 as was observed in other regions. This consistency is again explained by the theory of evaporative cooling as discussed earlier hence lower temperatures as observed in Emanuel, Grell and BM in the months of DJF. It is however not surprising that wet bias and a warmer bias was observed for the other months, this could be attributed to the complexity of climatic interactions in these rainy months.

Table 4.15: Mean bias (MB) for surface temperature (2010 - 2014) for convective schemes in comparison with CRU dataset over the Savannah region.

Scheme	DJF	MAM	JJA	SON	Annual
Grell	0.82	-0.81	-0.33	-0.47	-0.47
BM	0.23	-2.36	-2.81	-2.38	-2.37
Tiedtke	-2.04	-1.76	-1.82	-1.73	-1.73
KF	-1.71	-1.24	-1.16	-1.29	-1.29
Emanuel	0.55	-1.40	-1.53	-1.54	-1.54

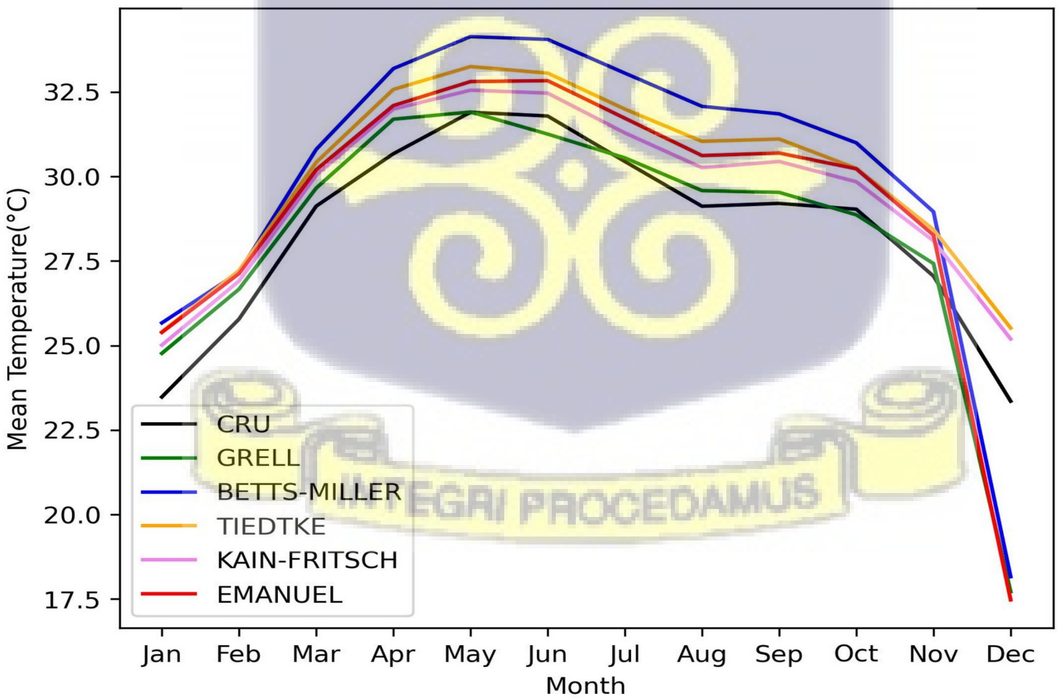

Figure 4.11: Mean surface temperature (°C) of Schemes over Savannah region in comparison with CRU observational data.

Table 4.16: RMSE and PCC for surface temperature (2010 - 2014) of the five (5) convective schemes in comparison with CRU dataset over the Savannah region

Scheme	DJF		MAM		JJA		SON		Annual	
	RMSE	PCC	RMSE	PCC	RMSE	PCC	RMSE	PCC	RMSE	PCC
Grell	4.76	0.79	3.43	0.89	3.18	0.92	3.12	0.89	3.12	0.89
BM	5.18	0.79	4.13	0.90	4.11	0.93	3.98	0.90	3.98	0.90
Tiedtke	4.41	0.86	3.79	0.89	3.52	0.93	3.56	0.90	3.56	0.90
KF	4.15	0.86	3.44	0.90	3.33	0.93	3.36	0.90	3.36	0.90
Emanuel	5.19	0.78	3.53	0.90	3.37	0.93	3.55	0.90	3.55	0.90

4.3.3 Relative Humidity

Good PCC values again are observed just as has been seen in the Guinean region and depicted in Figure 4.12 and Table 4.18. Overestimation of relative humidity has also been dominant in this region with Emanuel, BM and KF underestimating in some months. BM actually underestimated throughout the months of analysis agreeing with Figure 4.12. The general performance was good as shown in Figure 4.12, Table 4.17 and 4.18. Grell has on average dominated in performance except in the months of JJA where Emanuel edged (see Table 4.18). A simple comparison between relative humidity simulations and precipitation reveals a good correlation in this region as seen in Guinean coast.

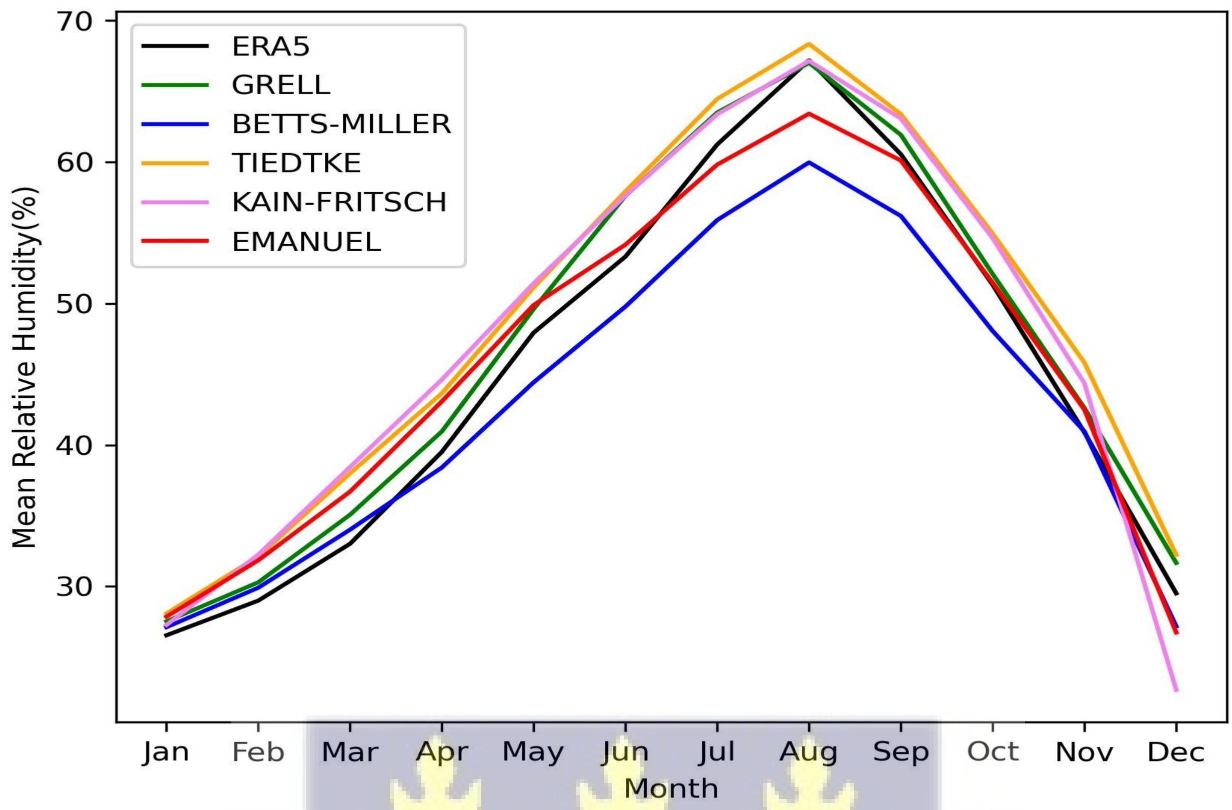

Figure 4.12: Mean relative humidity (%) of Schemes over Savannah region in comparison with ERA5 reanalysis data.

Table 4.17: Mean bias (MB) for relative humidity (2010 - 2014) for convective schemes in comparison with ERA5 dataset over the Savannah region

Scheme	DJF	MAM	JJA	SON	Annual
Grell	-1.48	-1.72	-2.12	-1.29	-1.65
BM	0.28	1.20	5.36	2.52	2.34
Tiedtke	-2.46	-4.11	-3.00	-3.80	-3.34
KF	0.95	-4.68	-2.13	-3.10	-2.24
Emanuel	-0.47	-3.07	1.45	-0.44	-0.63

Table 4.18: RMSE and PCC for relative humidity (2010 - 2014) of the five (5) convective schemes in comparison with ERA5 dataset over the Savannah region

Scheme	DJF		MAM		JJA		SON		Annual	
	RMSE	PCC	RMSE	PCC	RMSE	PCC	RMSE	PCC	RMSE	PCC
Grell	3.93	0.99	3.66	0.99	5.80	0.99	3.35	0.99	4.30	0.99
BM	3.69	0.98	5.41	0.99	7.67	0.99	4.60	0.99	5.54	0.99
Tiedtke	5.35	0.98	6.15	0.99	5.36	0.99	5.90	0.99	5.70	0.99
KF	6.33	0.95	7.51	0.98	5.47	0.98	5.19	0.99	6.19	0.98
Emanuel	4.50	0.97	6.35	0.98	5.24	0.99	3.56	0.99	4.98	0.99

4.4 Sahel Region

4.4.1 Precipitation

The temporal distribution of precipitation over the Sahel region for CRU, Grell, BM, Tiedtke, KF, and Emanuel is shown in Figure 4.13. Table 4.19 shows the corresponding mean bias (MB) for each study months (DJF, MAM, JJA, SON, and Annual). As observed over the Guinea coast and the Savannah, Grell profoundly overestimates precipitation in the Sahel region. The Sahel region also experiences overestimation from all schemes though to a lesser extend with Emanuel and BM. This behavior of BM and Emanuel was captured very well in Table 4.19 as they outperform all the other convective schemes. The greatest wet bias is 6.38 mm/day which was exhibited by Grell in the months of JJA. The RMSE column of Table 4.20 strengthens the results in Table 4.19: The RMSE values for Emanuel and BM has been relatively outstanding.

Table 4.19: Mean bias (MB) for precipitation (2010 - 2014) for convective schemes in comparison with CRU dataset over the Sahel region

Scheme	DJF	MAM	JJA	SON	Annual
Grell	-1.54	-5.05	-6.38	-6.33	-4.83
BM	-0.33	-0.93	-0.71	-0.33	-0.58
Tiedtke	-0.58	-2.41	-1.88	-2.04	-1.73
KF	-0.61	-2.08	-1.57	-1.47	-1.43
Emanuel	-0.28	-0.92	-0.78	-0.38	-0.59

Table 4.20: RMSE and PCC for precipitation (2010 - 2014) of the five (5) convective schemes in comparison with CRU dataset over the Sahel region

Scheme	DJF		MAM		JJA		SON		Annual	
	RMSE	PCC	RMSE	PCC	RMSE	PCC	RMSE	PCC	RMSE	PCC
Grell	3.71	0.72	7.70	0.76	9.14	0.69	10.94	0.69	8.31	0.72
BM	0.80	0.68	1.73	0.63	2.61	0.60	1.30	0.83	1.74	0.73
Tiedtke	1.62	0.60	4.14	0.61	4.03	0.59	3.76	0.75	3.54	0.68
KF	1.38	0.71	3.07	0.71	2.81	0.74	2.52	0.85	2.53	0.78
Emanuel	0.66	0.72	1.65	0.73	2.49	0.73	1.33	0.85	1.67	0.80

Emanuel produces the best MB and RMSE values of 0.28 mm/day and 0.66 mm/day respectively, both in the months of DJF. It is also not surprising to find Grell producing the worst RMSE value of 10.94 mm/day. Despite this discrepancy between the observation and schemes, they agree well with correlation greater than 0.67 over the entire West African Domain. The overestimation over Sahel region is largely supports the findings of (Adeniyi, 2014; Koné et al., 2018).

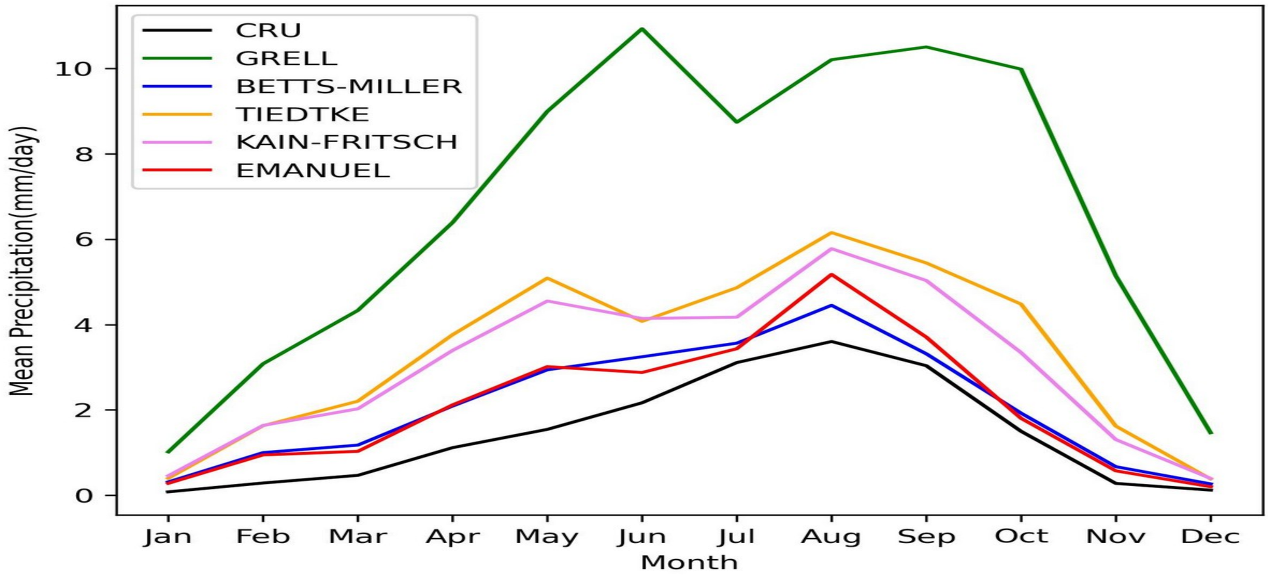

Figure 4.13: Mean precipitation (mm/day) of Schemes over Sahel region in comparison with CRU observational data.

4.4.2 Surface Temperature

Table 4.21 shows the the mean bias of the various convective schemes in relation to CRU. Overestimation was dominant again, with BM, Emanuel and Grell underestimating in the months DJF and Grell again in JJA and annually. This is evident from Figure 4.14. As discussed earlier, Grell outperforms in simulating surface temperature with the highest mean bias of 0.94 °C occurring in DJF and least of 0.14 °C in the annual analysis. BM produced the greatest mean bias of 2.25 °C in JJA. Table 4.22 presents the RMSE and the PCC.

Table 4.21: Mean bias (MB) for surface temperature (2010 - 2014) for convective schemes in comparison with CRU dataset over the Sahel region

Scheme	DJF	MAM	JJA	SON	Annual
Grell	0.94	-0.36	0.17	-0.19	0.14
BM	0.53	-1.81	-2.25	-1.83	-1.34
Tiedtke	-1.78	-1.29	-1.46	-1.39	-1.48
KF	-1.36	-0.77	-0.65	-0.91	-0.92
Emanuel	0.82	-1.08	-1.25	-1.17	-0.67

Table 4.22: RMSE and PCC for surface temperature (2010 - 2014) of the five (5) convective schemes in comparison with CRU dataset over the Sahel region

Scheme	DJF		MAM		JJA		SON		Annual	
	RMSE	PCC	RMSE	PCC	RMSE	PCC	RMSE	PCC	RMSE	PCC
Grell	4.67	0.86	3.44	0.93	3.25	0.94	3.15	0.93	3.68	0.92
BM	5.087	0.85	3.94	0.93	3.95	0.95	3.83	0.93	4.23	0.92
Tiedtke	4.39	0.91	3.69	0.93	3.45	0.95	3.55	0.93	3.79	0.93
KF	4.04	0.91	3.45	0.93	3.26	0.95	3.29	0.94	3.53	0.93
Emanuel	5.11	0.85	3.52	0.94	3.37	0.95	3.43	0.94	3.93	0.92

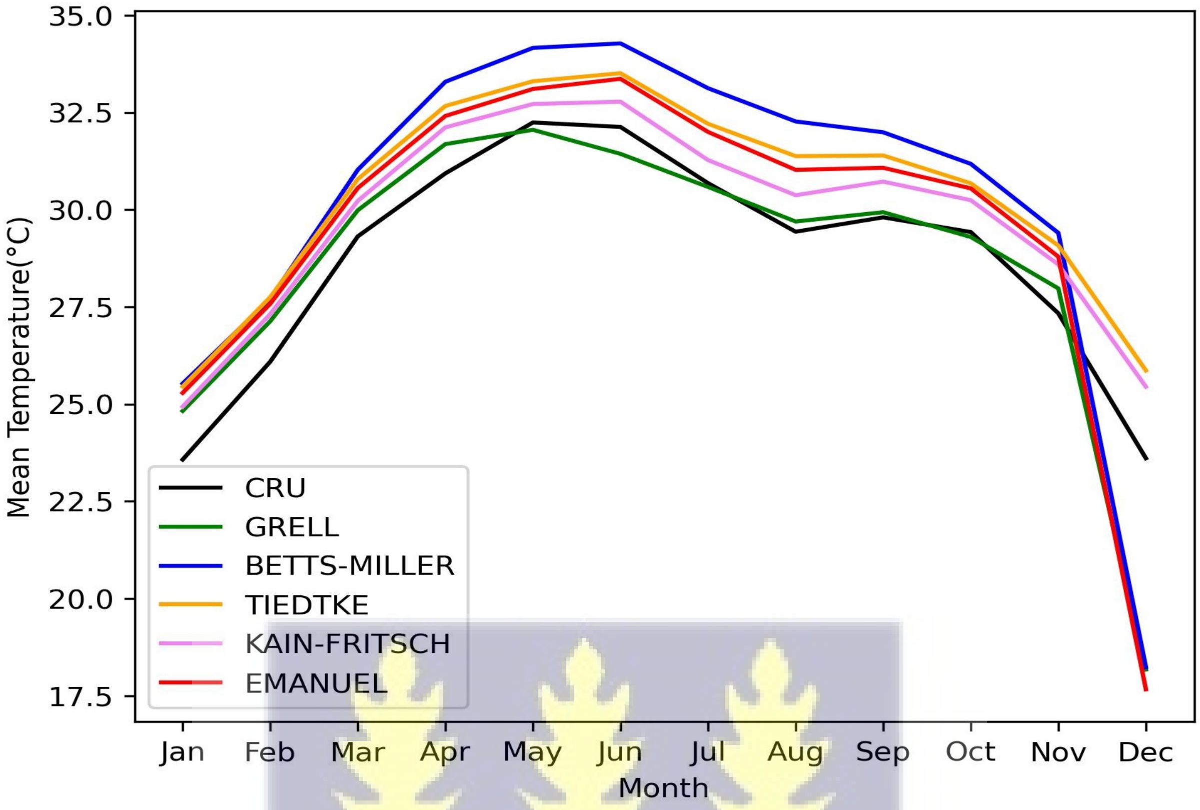

Figure 4.14: Mean surface temperature (°C) of Schemes over Sahel region in comparison with CRU observational data.

4.4.3 Relative Humidity

The dynamics observed over the Sahel region is not very different from what was discussed previously. Table 4.23 presents the mean bias of the various convective schemes and shows overestimation by most of the schemes except BM and KF in JJA and annually and DJF respectively. BM has consistently outperformed the rest except in JJA when it was outperformed by Emanuel (see Table 4.23 and 4.24). This may be due to the temperature dependence of the water content in the Emanuel scheme as JJA is a period where surface temperature drops.

Table 4.23: Mean bias (MB) for relative humidity (2010 - 2014) for convective schemes in comparison with ERA5 dataset over the Sahel region

Scheme	DJF	MAM	JJA	SON	Annual
Grell	-1.75	-5.19	-3.53	-3.33	-3.45
BM	-0.36	-1.90	3.14	-0.19	0.18
Tiedtke	-2.49	-6.75	-4.41	-5.48	-4.78
KF	0.53	-8.13	-4.35	-5.18	-4.28
Emanuel	-0.54	-5.36	-0.17	-2.51	-2.15

Table 4.24: RMSE and PCC for relative humidity (2010 - 2014) of the five (5) convective schemes in comparison with ERA5 dataset over the Sahel region

Scheme	DJF		MAM		JJA		SON		Annual	
	RMSE	PCC	RMSE	PCC	RMSE	PCC	RMSE	PCC	RMSE	PCC
Grell	4.90	0.98	7.26	0.98	6.75	0.98	5.32	0.99	6.14	0.98
BM	4.24	0.98	5.52	0.98	6.36	0.99	3.77	0.99	5.08	0.98
Tiedtke	5.79	0.97	9.14	0.97	6.71	0.99	7.60	0.98	7.41	0.98
KF	6.89	0.94	10.90	0.96	7.45	0.98	7.23	0.98	8.28	0.97
Emanuel	5.09	0.96	7.90	0.98	5.28	0.99	4.58	0.99	5.86	0.98

The dynamics observed over the Sahel region is not very different from what was discussed previously. Table 4.23 presents the mean bias of the various convective schemes and shows overestimation by most of the schemes except BM and KF in JJA and annually and DJF respectively. BM has consistently outperformed the rest except in JJA when it was outperformed by Emanuel (see Table 4.23 and 4.24). This may be due to the temperature dependence of the water content in the Emanuel scheme as JJA is a period where surface temperature drops.

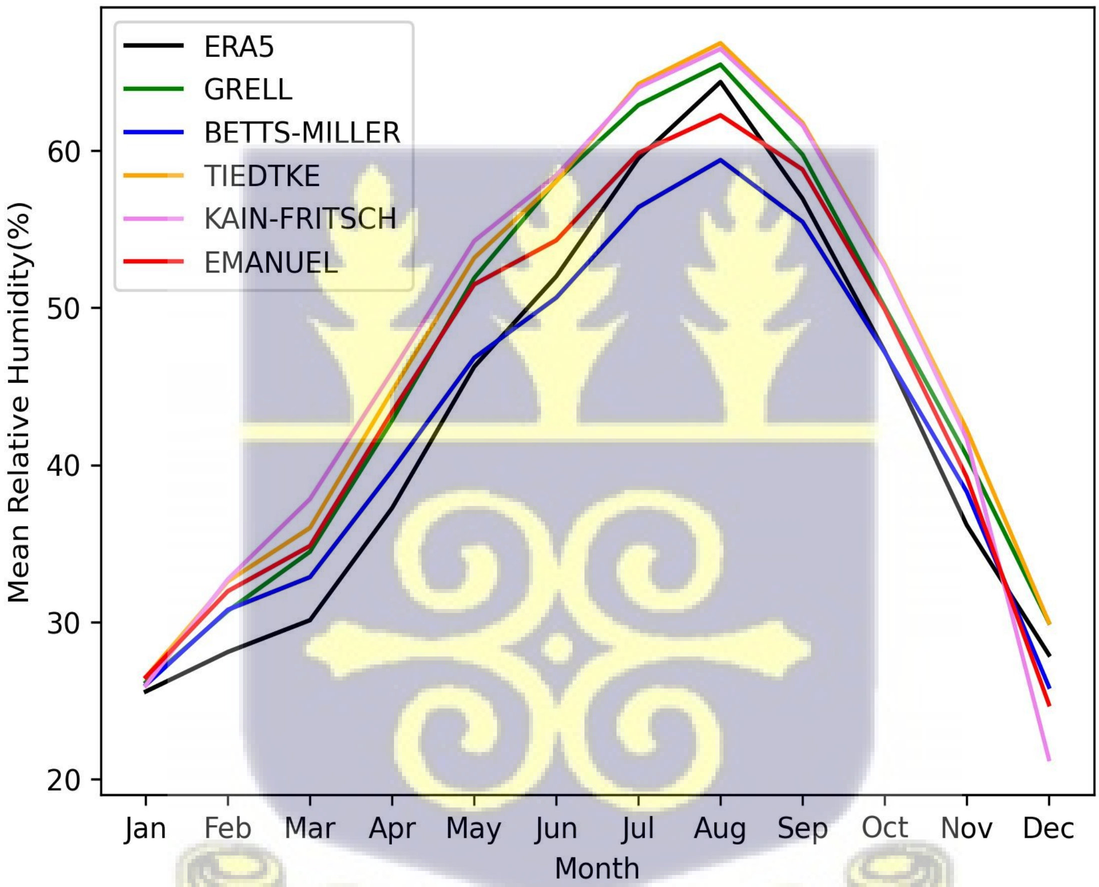

Figure 4.15: Mean relative humidity (%) of Schemes over Sahel region in comparison with ERA5 reanalysis data.

4.5 JJA Analysis

The dynamics across the various sub-regions in the months of JJA is analyzed here. This is done because JJA coincides more appropriately with the local monsoon months than DJF, MAM or SON hence is important to access the performance of the various schemes over the sub-regions of the study.

4.5.1 Precipitation

The spatial distribution of precipitation for the season of JJA is shown Figure 4.16. It is quite evident here that Grell overestimate precipitation relative to CRU observational data. Emanuel and BM shows mild overestimation relative to Grell, Tiedtke and KF.

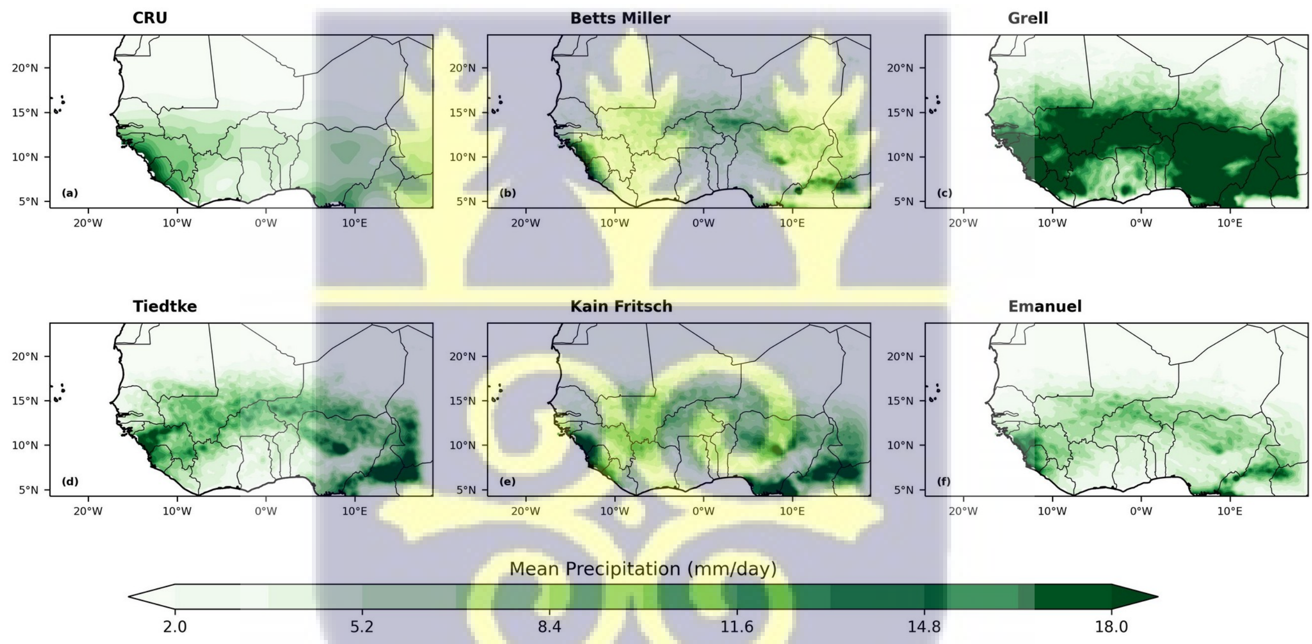

Figure 4.16: Spatial distribution of mean precipitation (mm/day) of Schemes over West Africa in comparison with CRU observational data for JJA.

Table 4.25: RMSE and MB for JJA precipitation (2010 - 2014) of the five (5) convective schemes in comparison with CRU dataset over sub-regions of the study domain.

	Grell		BM		Tiedtke		KF		Emanuel	
	RMSE	BIAS	RMSE	BIAS	RMSE	BIAS	RMSE	BIAS	RMSE	BIAS
GC	11.04	-7.81	3.59	1.16	3.79	-1.3	2.91	-0.62	2.61	0.16
Sav	8.9	-6.38	2.2	-0.26	3.56	-1.76	2.76	-1.46	2.36	-0.78
Sah	9.14	-6.38	2.61	-0.71	4.03	-1.88	2.81	-1.57	2.49	-0.78
WA	13.11	-6.99	3.54	-0.59	4.91	-1.86	4.3	-1.67	3.26	-0.79

Table 4.25 presents the the statistical metrics (RMSE and mean bias) that indicates the performance of the five convective schemes over the Guinea Coast (GC), the Savannah region (Sav), the Sahel region (Sah) and the West African domain. It is noticed that all schemes performed better in the sub-regions (GC, Sav and Sah) as compared to the West African (WA) domain except BM (see Table 4.25, the RMSE column). All schemes also simulated precipitation better in the Savannah (Sav) and Sahel (Sah) regions compared to the Guinea Coast (GC). This maybe due to the complex dynamics observed in the Guinea Coast such as very complex terrains, direct interactions with the Atlantic Ocean and many more. Figure 4.17 comes in with the PCC and the normalized standard deviation of all schemes over the West African domain and its sub-regions. It is again noticed that all schemes had PCC and standard deviations that compare well with those of the other sub-regions for the months of JJA and in comparison with CRU observational dataset. Model standard deviations are normalized by their respective means. The taylor diagram indicates a relatively good PCC for all schemes over the Savannah region and the Guinea Coast. In each region except Savannah region, Emanuel has produced good PCC than others.

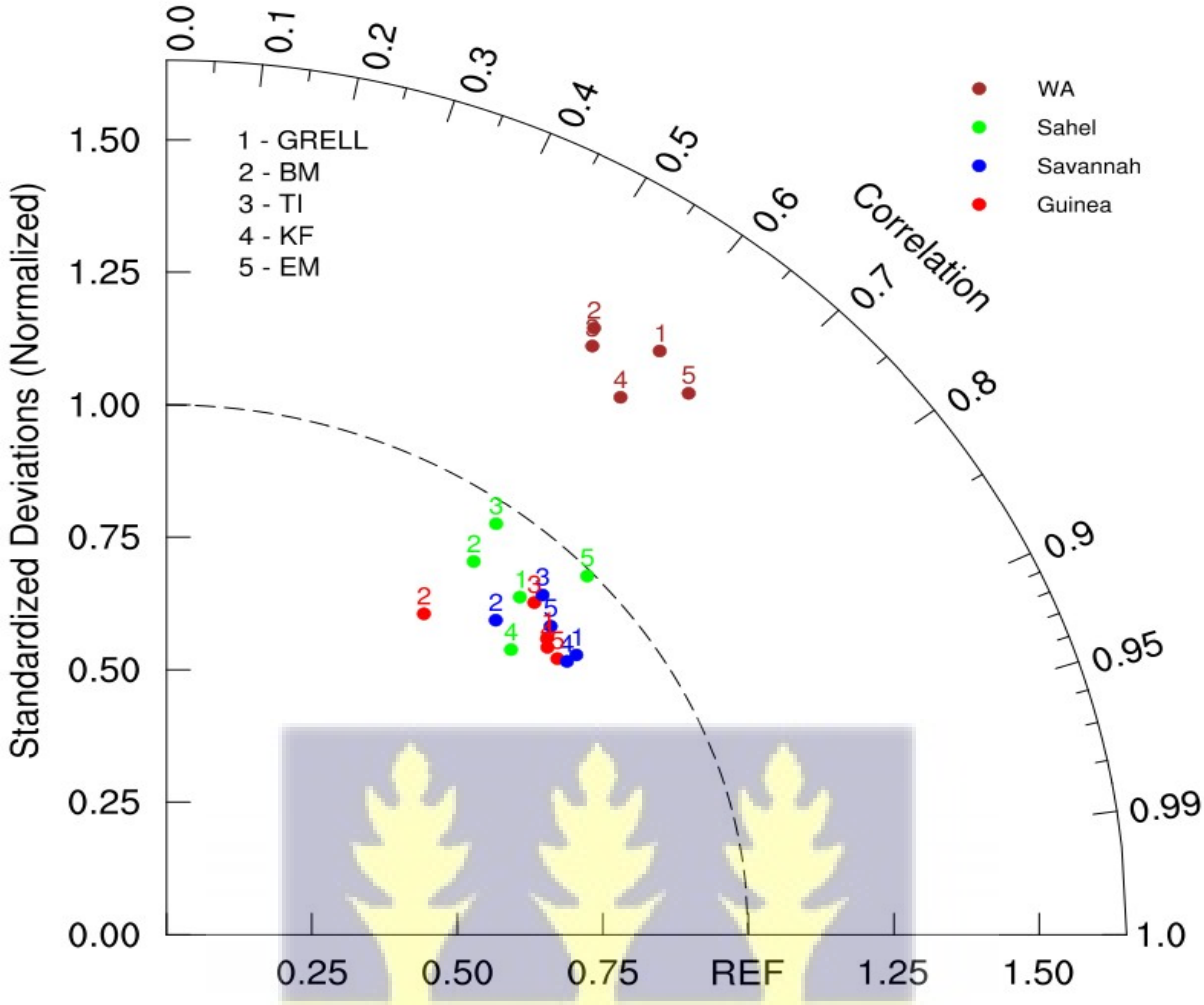

Figure 4.17: Taylor diagram showing the pattern correlation and the standard deviation (normalized) of the five convective schemes over the West Africa (WA) and its sub-regions (GC, Sav, Sah) for the months of JJA

4.5.2 Surface Temperature

Table 4.26: RMSE and MB for JJA surface temperature (2010 - 2014) of the five (5) convective schemes in comparison with CRU dataset over sub-regions of the study domain.

	Grell		BM		Tiedtke		KF		Emanuel	
	RMSE	BIAS	RMSE	BIAS	RMSE	BIAS	RMSE	BIAS	RMSE	BIAS
GC	3.54	-0.29	4.23	-2.60	3.74	-1.77	3.55	-1.29	3.61	-1.48
Sav	3.18	-0.33	4.11	-2.81	3.52	-1.82	3.33	-1.16	3.37	-1.53
Sah	3.25	0.17	3.95	-2.25	3.45	-1.46	3.26	-0.65	3.37	-1.25
WA	12.85	-5.16	13.36	-6.65	13.15	-6.15	12.73	-5.59	12.80	-5.86

The results for the five convective schemes over the various sub-regions of the West African domain is presented in Table 4.26. The RMSE for Grell stands out in the sub-regions except the West African domain. Figure 4.18 shows a good simulation of the meridional surface temperature transition zone between the Guinean Coast and the Savannah region. The importance of this is discussed in Koné et al., (2018). The spatial mean bias for JJA averaged over time is illustrated in Figure 4.19. It is evident here again that the model is dominantly warm bias. Grell and to a lesser extent KF produces cold bias around northern Savannah to central Sahel consistent with Kouassi et al., (2022). Emanuel and Tiedtke has similar profiles except the density around the coasts of Southern West Africa. All schemes produced cold bias to varying degree over the Guinean highlands.

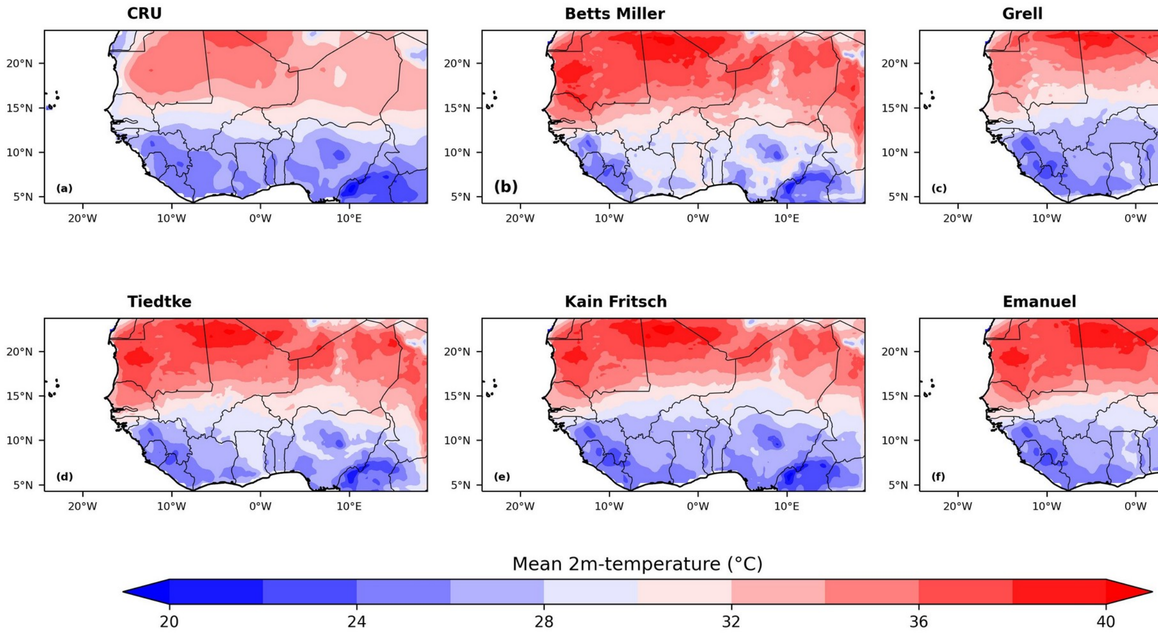

Figure 4.18: Spatial distribution of mean JJA surface temperature (°C) of Schemes over West Africa in comparison with CRU observational data for JJA.

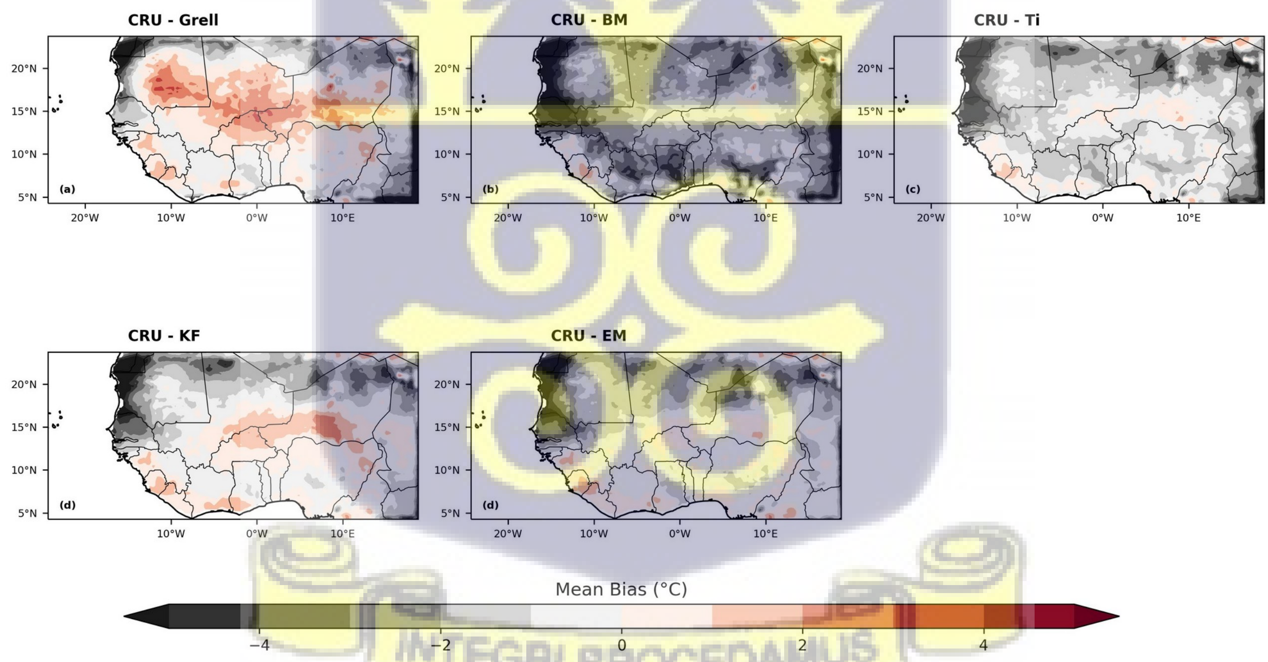

Figure 4.19: Distribution of spatial mean bias (°C) indicating the performance of Convective Schemes over West Africa in comparison with CRU observational dataset for JJA.

4.5.3 Relative Humidity

The RMSE and mean bias is presented in Table 4.27. Tiedtke and Emanuel performed relatively well as discussed in subsection 4.5.2. There is also a great difference in the performance of each scheme in the sub-regions as compared with the entire domain.

Table 4.27: RMSE and MB for JJA relative humidity (2010 - 2014) of the five (5) convective schemes in comparison with ERA5 dataset over sub-regions of the study domain.

	Grell		BM		Tiedtke		KF		Emanuel	
	RMSE	BIAS	RMSE	BIAS	RMSE	BIAS	RMSE	BIAS	RMSE	BIAS
GC	5.48	-1.25	7.59	5.34	3.86	-2.12	4.28	-1.22	4.18	1.3
Sav	5.8	-2.12	7.67	5.36	5.36	-3	5.47	-2.13	5.25	1.45
Sah	6.75	-3.53	6.36	3.14	6.71	-4.41	7.45	-4.35	5.28	-0.17
WA	24.05	-10.77	23.27	-6.21	24.8	-11.25	25.23	-11.22	23.92	-8.4

4.6 Perturbed Emanuel Scheme

Four (4) control parameters of the Emanuel scheme stochastically were perturbed as described in chapter three (3) of this thesis. The results are discussed here as follows:

4.6.1 Precipitation

Table 28 presents the mean bias over the climatic sub-regions of West Africa. The results achieved here shows that the perturbations are more sensitive to "temporal" change rather than "spatial" change. This is expected from the results of Kuell & Bott, (2014) and Griffin et al., (2020). The unperturbed mean bias is considerably higher than all the perturbed ensemble members over the GC. This is good because the GC is known to be an important climatic zone in West Africa. The Sav, Sah saw no clear improvement of the statistical bias. This maybe due to the inter-dependence of the perturbed parameters (Bowler et al., 2008).

Table 4.28: Mean bias (mm/day) of perturbed and unperturbed Emanuel scheme over GC, Sav, Sah and WA in comparison with CRU observational dataset.

Zones	Unperturbed Bias	Mix1 Bias	Mix2 Bias	Mix3 Bias	Mix4 Bias
GC	0.16	0.07	0.09	0.08	0.1
Sav	-0.78	-0.8	-0.75	-0.8	-0.78
Sah	-0.78	-0.8	-0.77	-0.79	-0.78
WA	-0.79	-0.83	-0.82	-0.83	-0.82

As mentioned earlier, it is essential to verify that the quality of the convective parameterization scheme and hence the model is preserved or improved. The mean bias of the ensemble mean and the unperturbed is now examined over the study period. Both produces a wet bias but to different extends. The perturbed ensemble mean positively improves the model results right from January to

December by producing a more accurate simulation of precipitation (dryer bias compared to unperturbed). The difference between the mean biases (see Figure 4.20) is significant and may be attributed to the fact that the extremes of the parameter values were rigorously explored. This was carefully selected to give a large perturbation which will result in each parameter assuming a value that is near the extremes (V_{min} and V_{max}) of what it can be physically assigned. While the perturbed ensemble mean produced approximately a flat mean bias curve between April and May, the unperturbed plunges further thus overestimating compared to the perturbed ensemble mean. A similar behavior is observed in August through to October. Both periods are dominated by small scale features since April to October represents the onset, peak and end of the wet period over West Africa (Sultan et al., 2003). During this wet periods, convective activity in the Inter-tropical Convergence Zone (ITCZ) is significantly enhanced hence making it difficult for parameterizations to capture. This makes it interesting for the perturbed ensemble mean to capture this complexity fairly well.

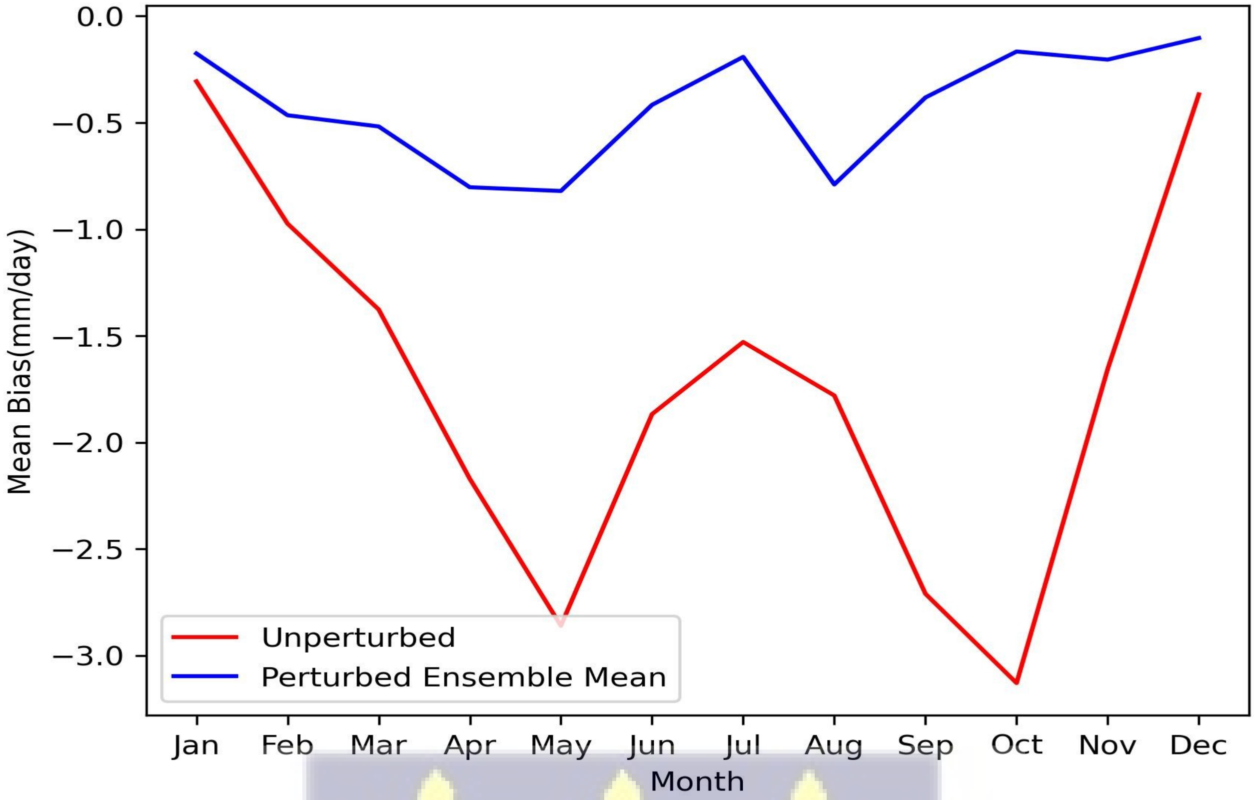

Figure 4.20: Mean bias (mm/day) of perturbed ensemble mean against unperturbed Emanuel convective scheme over the study period in comparison with CRU observational data.

The closing up of mean bias values between November and February is expected due to the fall in the rigour of convection. One can not question the significant deviation of control and ensemble mean biases even in dry months; this is because the perturbations are not limited temporally or spatially, once perturbed the model does not defaults. The error between both simulations (perturbed ensemble mean and unperturbed) is illustrated in Figure 4.21.

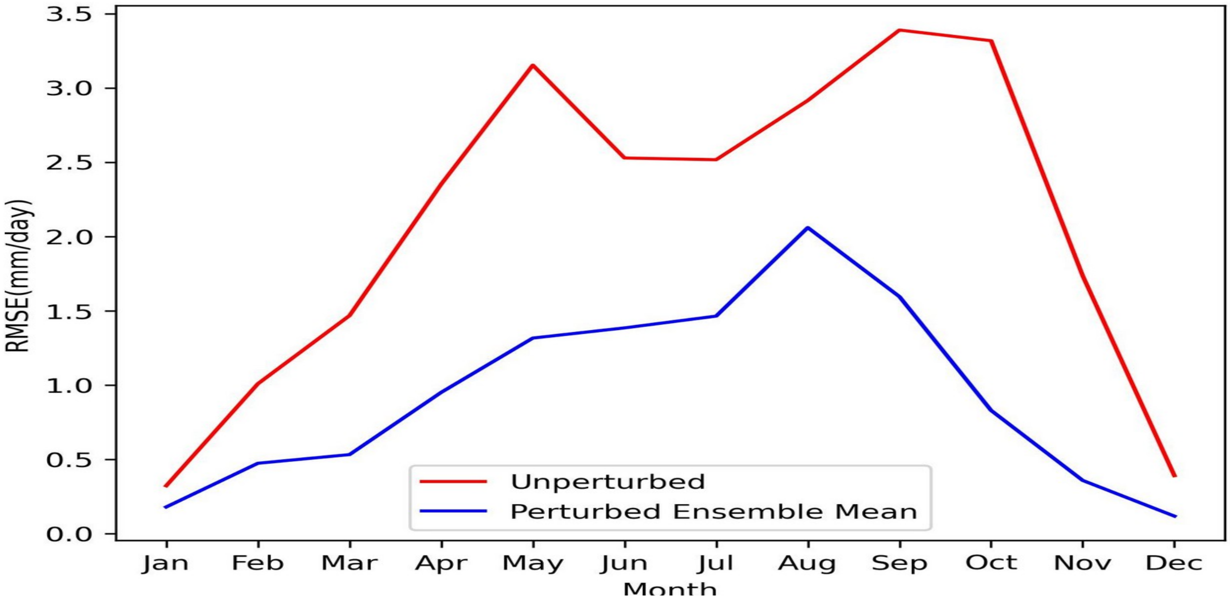

Figure 4.21: RMSE (mm/day) of perturbed ensemble mean against unperturbed Emanuel convective scheme over the study period in comparison with CRU observational data.

Figure 4.21 shows an improvement in the RMSE compared to CRU observational dataset. It is important to mention that despite the improvement, the perturbation is of similar quality as the unperturbed model. The uncertainties of the scheme is quantified by the RMSE. The standard deviation of the perturbed ensemble mean, the unperturbed and the observational dataset is compared in Figure 4.22. It is observed that the spread of the unperturbed Emanuel scheme has been improved relative to CRU. The spread between perturbed and unperturbed is closest around August. This may still be attributed to the difficulty explained above.

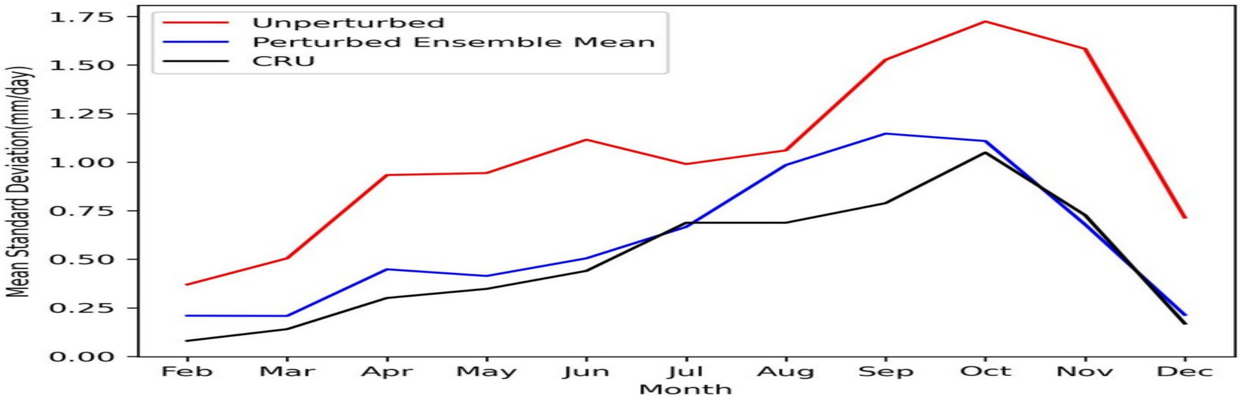

Figure 4.22: Standard deviation (mm/day) of perturbed ensemble mean, unperturbed Emanuel convective scheme against the observed precipitation (CRU)

4.6.2 Surface Temperature

The mean bias over climatic sub-regions of West Africa is presented in Table 4.29. The results shown in Table 4.29 and Figure 4.23 – 4.25 signifies that the perturbed ensemble mean does not significantly depart from the unperturbed unlike what was discussed for precipitation. This does not come as a surprise, perturbing scheme parameters in the way described above changes the physical "pedestal" of the scheme. This may favor some variables like precipitation due to its heavy dependence on atmospheric micro-physics (Emanuel, 1997; Emanuel & Živković-Rothman, 1999).

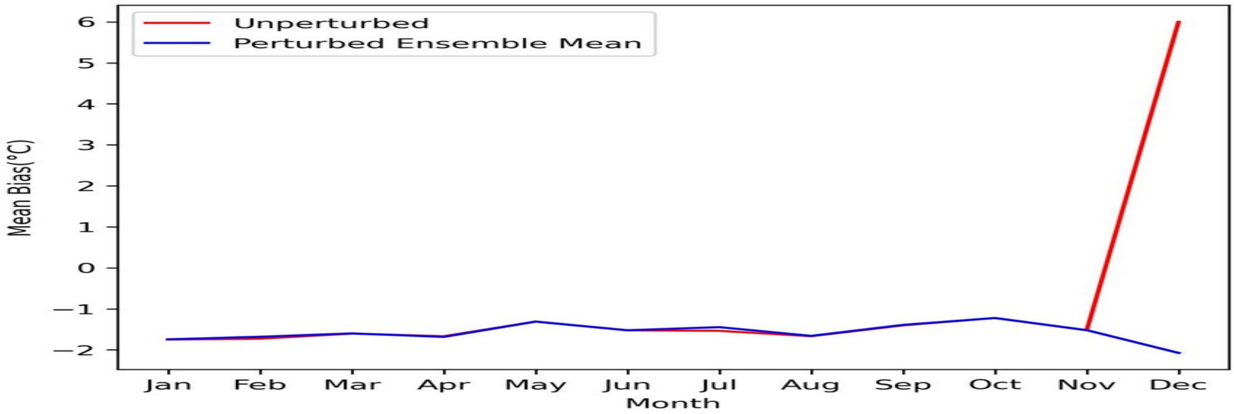

Figure 4.23: Mean bias (°C) of perturbed ensemble mean against unperturbed Emanuel convective scheme over the study period in comparison with CRU observational data.

Table 4.29: Mean bias (°C) of perturbed and unperturbed Emanuel scheme over GC, Sav, Sah and WA in comparison with CRU observational dataset.

Zones	Unperturbed Bias	Mix1 Bias	Mix2 Bias	Mix3 Bias	Mix4 Bias
GC	-1.48	-1.45	-1.46	-1.45	-1.45
Sav	-1.53	-1.49	-1.5	-1.49	-1.5
Sah	-1.25	-1.21	-1.21	-1.21	-1.21
WA	-5.86	-5.84	-5.84	-5.83	-5.8

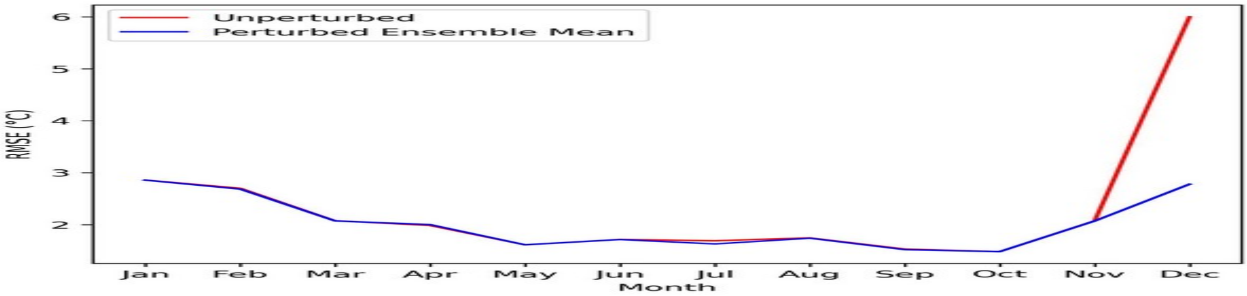

Figure 4.24: RMSE (°C) of perturbed ensemble mean against unperturbed Emanuel convective scheme over the study period in comparison with CRU observational data.

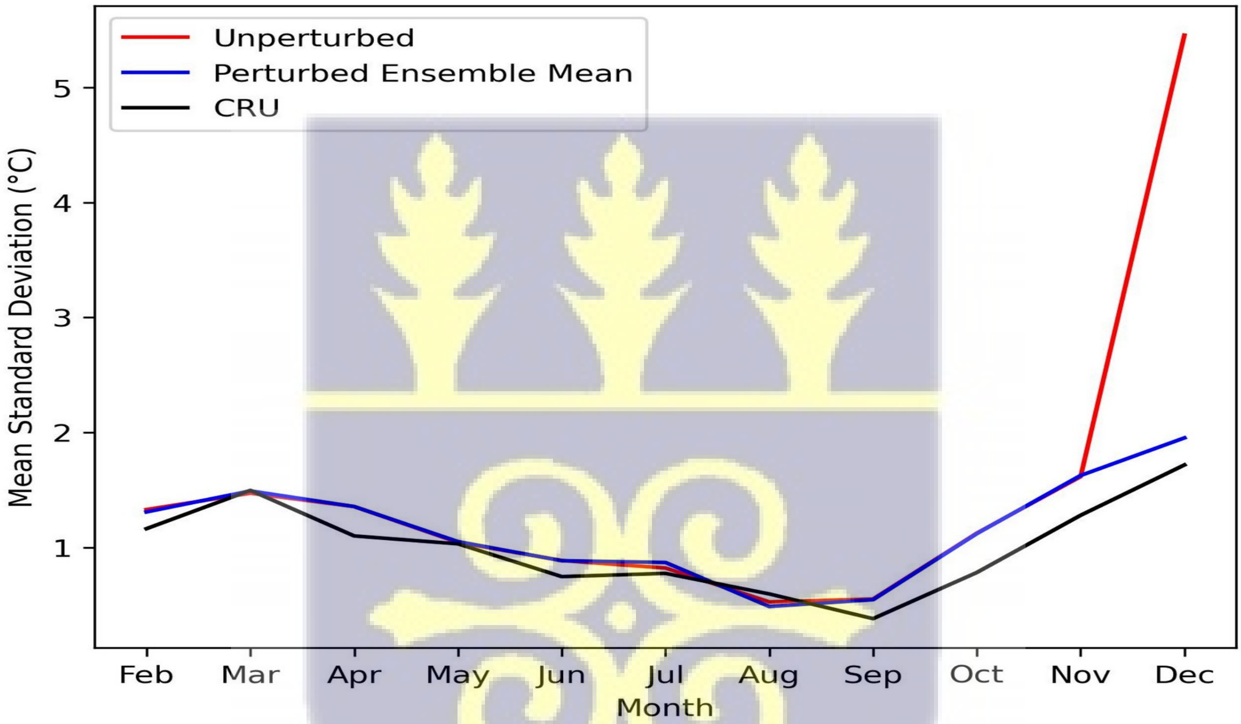

Figure 4.25: Standard deviation (°C) of perturbed ensemble mean, unperturbed Emanuel convective scheme against the observed precipitation (CRU)

CHAPTER FIVE

5.0 CONCLUSIONS

5.1 Sensitivity Study

Five convective parameterization schemes (Grell, Emanuel, BM, Tiedtke,KF) were evaluated against the CRU observational dataset for the months of DJF, MAM, JJA and SON. The sensitivities of these schemes have been discussed for each of the three variables (precipitation, surface temperature and relative humidity) across the three main climatic zones (Guinea coast, Savannah region, Sahel region and over West Africa). The behaviors and the manner in which all five schemes simulate precipitation, temperature and humidity over West Africa is not very different from in the sub-regions, their precision however increases for all climate variables over the sub-regions. Overestimation is a dominant feature observed in this study: Emanuel and to a lesser extent BM performs better in simulating precipitation; Grell and to a lesser extent Emanuel produces the best performance for temperature with an intermittent performance from KF. Relative humidity has been cumbersome to simulate, this was shown as different schemes performed better in different zones and this is to be expected: Emanuel and BM outperforms KF, Grell and Tiedtke over the West African domain; Gell and Tiedtke outperformed the rest in the Guinea region; Grell and BM outperforming in the Savannah and Sahel regions respectively. It is important to note that all schemes had excellent correlations and Emanuel has always had an intermittent performance in the simulation of relative humidity. The various performance was again analyzed for the months of JJA since it by large coincides with the monsoon months of West Africa. Emanuel simulated precipitation better for GC, Sah and WA except Sav where BM outperformed it. Grell was outstanding in the simulation of surface temperature over all sub-regions but over the WA where Emanuel edged. Relative humidity again was simulated better by different scheme over different regions: Tiedtke in the GC, Emanuel in the Sav and Sah regions an BM over the WA region. The results obtained here satisfies the first objectives of this study.

5.2 Stochastic Perturbation

The Emanuel scheme control parameters were then perturbed and the mean of the perturbed ensemble and the control (unperturbed) both compared to the CRU observational dataset over the study period: mean biases of the unperturbed scheme precipitation was improved by the perturbation which translated into better RMSE and spread. The perturbations did not favor surface temperature but did not degrade the simulation too. This is first in line of several research that seeks to use stochastic perturbation to improve forecasts.

RECOMMENDATIONS

For future studies of stochastic related perturbations and optimizing CPS, it is recommended that:

1. A larger ensemble size should be used in future studies.

2. Involve the perturbation of the control parameters of the large scale precipitation scheme (SUBEX) and the cloud microphysics schemes.

3. Capture small scale and sub-grid variability by adding a stochastic white noise to appropriate CPS parameters such as the mixing rates of cloud air and environmental air.

REFERENCES

1. A. Slingo. (1988). A GCM Parameterization for the Shortwave Radiative Properties of Water Clouds. *Journal of Atmospheric Sciences*, *46*(10), 1419–1427. https://doi.org/https://doi.org/10.1175/1520-0469(1989)046%3C1419:AGPFTS%3E2.0.CO;2

2. Adeniyi, M. O. (2014). Sensitivity of different convection schemes in RegCM4.0 for simulation of precipitation during the Septembers of 1989 and 1998 over West Africa. *Theoretical and Applied Climatology*, *115*(1–2), 305–322. https://doi.org/10.1007/s00704-013-0881-5

3. Ali, S., Dan, L., Fu, C., & Yang, Y. (2015). Performance of convective parameterization schemes in Asia using RegCM: Simulations in three typical regions for the period 1998–2002. *Advances in Atmospheric Sciences*, *32*(5), 715–730. https://doi.org/10.1007/s00376-014-4158-4

4. Arakawa, A. (2004). The cumulus parameterization problem: Past, present, and future. *Journal of Climate*, *17*(13), 2493–2525. https://doi.org/10.1175/1520-0442(2004)017<2493:RATCPP>2.0.CO;2

5. Betts, A. K. (1986). *A new convective adjustment scheme. Part I: Observational and theoretical basis* (pp. 677–691). https://alanbetts.com/workspace/uploads/betts-connvectiveadjust-qj86-1276985317.pdf

6. Betts, K., Centre, E., Weather, M., Reading, F., & United, B. (1993). *Chapter 9 The Betts-Miller Scheme*. 107–108.

7. Blyth, A. M. (1993). Entrainment in Cumulus Clouds. *Journal of Applied Meteorology*, *32*, 626–641. https://doi.org/https://doi.org/10.1175/1520-0450(1993)032%3C0626:EICC%3E2.0.CO;2

8. Bowler, N. E., Arribas, A., Mylne, K. R., Robertson, K. B., & Beare, S. E. (2008). The MOGREPS Short-Range Ensemble Preiction System. *Royal Meteorological Society*, 703–722. https://doi.org/10.1002/qj

9. Charney, J. G., & Elliassen, A. (1963). On the Growth of the Hurricane Depresion. *Journal of the Atmospheric Sciences*, *21*(1), 68–75. https://doi.org/https://doi.org/10.1175/1520-0469(1964)021%3C0068:OTGOTH%3E2.0.CO;2

10. Deshpande, M. S., Pattnaik, S., & Salvekar, P. S. (2012). Impact of cloud parameterization on the numerical simulation of a super cyclone. *Annales Geophysicae*, *30*(5), 775–795. https://doi.org/10.5194/angeo-30-775-2012

11. Dickinson, R. E. (1989). National Center for Atmospheric Research*, Boulder, CO 80307-3000, U.S.A. *Atmospheric Research*, 383–384.

12. Elguindi, N., Bi, X., Giorgi, F., Nagarajan, B., Pal, J., Solmon, F., Rauscher, S., & Zakey, A. (2006). *User ' s Guide*. *May*, 1–58.

13. Elguindi, N., Bi, X., Giorgi, F., & others. (2011). Regional climate model RegCM user manual 4.7. *ITCP, Trieste, Italy, May*, 32p.

14. Emanuel, K. A. (1991). A Scheme for Representing Cumulus Convection in Large-Scale Model. *Journal of the Atmospheric Sciences*, *48*, 2313–2335.

15. Emanuel, K. A. (1997). The Problem of Convective Moistening. *The Physics and Parameterization of Moist Atmospheric Convection*, 447–461. https://doi.org/10.1007/978-94-015-8828-7_18

16. Emanuel, K. A., & Živković-Rothman, M. (1999). Development and evaluation of a convection scheme for use in climate models. *Journal of the Atmospheric Sciences*, *56*(11), 1766–1782. https://doi.org/10.1175/1520-0469(1999)056<1766:DAEOAC>2.0.CO;2

17. Flatoy, F. (1992). Comparison of two parameterization schemes for cloud and precipitation processes. *Tellus, Series A-B, 44 A*(1), 41–53. https://doi.org/10.3402/tellusa.v44i1.14942

18. Giorgi, F., & Bates, G. T. (1989). The Climatological Skill of a Regional Model Over Complex Terrain. *American Meteoroological Society*, *4*(1), 2325–2347. https://www.ptonline.com/articles/how-to-get-better-mfi-results

19. Giorgi, F., Maria, M. R., & Bates, G. T. (1993). Development of a Second -Generation Regional Climate Model (RegCM2) Part I. *Monthly Weather Review*, *121*(10), 2794–2813. https://doi.org/https://doi.org/10.1175/1520-0493(1993)121<2794:DOASGR>2.0.CO;2

20. Giorgi, F., Solmon, F., & Giuliani, G. (2016). Regional Climatic Model RegCM User ' s Guide. *International Centre for Theoretical Physics*, *May*, 1–57.

21. Goosse, H., Barriat, P. Y., Lefebvre, W., Loutre, M. F., & Zunz, V. (2010). Chapter 3 . Modelling the climate system. *Introduction to Climate Dynamics and Climate Modelling*, 59–86.

22. Grandpeix, J. Y., Phillips, V., & Tailleux, R. (2004). Improved mixing representation in Emanuel's convection scheme. *Quarterly Journal of the Royal Meteorological Society*, *130 C*(604), 3207–3222. https://doi.org/10.1256/qj.03.144

23. Grell, G. A. (1993). Prognostic Evaluation of Assumptions Used by Cumulus Parameterizations. *Monthly Weather Review*, *121*(3), 764–787. https://doi.org/https://doi.org/10.1175/1520-0493(1993)121<0764:PEOAUB>2.0.CO;2

24. Grell, G. A., Dudhia, J., & Stauffer, D. R. (1995). A Description of the Fifth-Generation Penn State/NCAR Mesoscale Model (MM5). *Atmospheric Research*, *June*. http://danida.vnu.edu.vn/cpis/files/Books/MM5 Discription - 1995.pdf

25. GRIFFIN, S. M., OTKIN, J. A., THOMPSON, G., FREDIANI, M., BERNER, J., & KONG, F. (2020). Assessing the impact of stochastic perturbations in cloud microphysics using GOES-16

infrared brightness temperatures. *Monthly Weather Review*, *148*(8), 3111–3137. https://doi.org/10.1175/MWR-D-20-0078.1

26. Kain, J. S., & Fritsch, J. M. (1990). A One-Dimensional Entraining/Detraining Plume Model and Its Application in Convective Parameterization. *Journal of the Atmospheric Sciences*, *47*(23), 2784–2802. https://doi.org/https://doi.org/10.1175/1520-0469(1990)047%3C2784:AODEPM%3E2.0.CO;2

27. Komkoua Mbienda, A. J., Guenang, G. M., Tanessong, R. S., Ashu Ngono, S. V., Zebaze, S., & Vondou, D. A. (2021). Possible influence of the convection schemes in regional climate model RegCM4.6 for climate services over Central Africa. *Meteorological Applications*, *28*(2), 1–17. https://doi.org/10.1002/met.1980

28. Koné, B., Diedhiou, A., Touré, N. E., Sylla, M. B., Giorgi, F., Anquetin, S., Bamba, A., Diawara, A., & Kobea, A. T. (2018). Sensitivity study of the regional climate model RegCM4 to different convective schemes over West Africa. *Earth System Dynamics*, *9*(4), 1261–1278. https://doi.org/10.5194/esd-9-1261-2018

29. Kouassi, A. A., Kone, B., Silue, S., Dajuma, A., N'datchoh, T. E., Adon, M., Diedhiou, A., & Yoboue, V. (2022). Sensitivity Study of the RegCM4's Surface Schemes in the Simulations of West Africa Climate. *Atmospheric and Climate Sciences*, *12*(01), 86–104. https://doi.org/10.4236/acs.2022.121007

30. Kuell, V., & Bott, A. (2014). Stochastic parameterization of cloud processes. *Atmospheric Research*, *143*, 176–197. https://doi.org/10.1016/j.atmosres.2014.01.027

31. Meinke, I., Roads, J., & Kanamitsu, M. (2007). *Evaluation of RSM-Simulated Precipitation During CEOP*. *85*, 145–166.

32. Of, J., Meteorology, A., & Studies, M. M. (2004). The Kain–Fritsch Convective Parameterization: An Update. *Journal of Applied Meteorology and Climatology*, *43*(1), 170–181. https://doi.org/https://doi.org/10.1175/1520-0450(2004)043<0170:TKCPAU>2.0.CO;2

33. Pal, J. S., Giorgi, F., Bi, X., Elguindi, N., Solmon, F., Gao, X., & Rauscher. S.A. (2007). Climate for the Developing. *Bulletin of the American Meteorological Society*, *88(9)*, 1395–1409.

34. Plant, R. S., & Yano, J.-I. (2015). *Parameterization of Atmospheric Convection* (Vol. 1). https://www.worldscientific.com/worldscibooks/10.1142/p1005

35. Raj Tiwari, P., Chandra Kar, S., Charan Mohanty, U., Dey, S., Sinha, P., Raju, P. V. S., & Shekhar, M. S. (2015). The role of land surface schemes in the regional climate model (RegCM) for seasonal scale simulations over Western Himalaya. *Atmósfera*, *28*(2), 129–142. https://doi.org/10.1016/s0187-6236(15)30005-9

36. Raymond, D. J. (1956). *Chapter 4 Simple models of Convection*. *0*, 53–71.

37. Sultan, B., Janicot, S., & Diedhiou, A. (2003). The West African monsoon dynamics. Part I: Documentation of intraseasonal variability. *Journal of Climate*, *16*(21), 3389–3406. https://doi.org/10.1175/1520-0442(2003)016<3389:TWAMDP>2.0.CO;2

38. Sundqvist, H., Berge, E., & Kristjansson, J. E. (1989). Condensation and cloud parameterization studies with a mesoscale numerical weather prediction model. *Monthly Weather Review*, *117*(8), 1641–1657. https://doi.org/10.1175/1520-0493(1989)117<1641:CACPSW>2.0.CO;2

39. Telford, J. W. (1975). Turbulence, entrainment, and mixing in cloud dynamics. *Pure and Applied Geophysics PAGEOPH*, *113*(1), 1067–1084. https://doi.org/10.1007/BF01592975

40. THOMPSON, G., BERNER, J., FREDIANI, M., OTKIN, J. A., & GRIFFIN, S. M. (2021). A stochastic parameter perturbation method to represent uncertainty in a microphysics scheme. *Monthly Weather Review*, *149*(5), 1481–1497. https://doi.org/10.1175/MWR-D-20-0077.1

41. Tiedtke, M. (1989). A Comprehensive Mass Flux Scheme for Cumulus Parameterization in Large-Scale Models. *Monthly Weather Review*, *117*(8), 1779–1800. https://doi.org/https://doi.org/10.1175/1520-0493(1989)117<1779:ACMFSF>2.0.CO;2

42. Villalba-Pradas, A., & Tapiador, F. J. (2022). Empirical values and assumptions in the convection schemes of numerical models. *Geoscientific Model Development*, *15*(9), 3447–3518. https://doi.org/10.5194/gmd-15-3447-2022

43. Wang, Y., Leung, L. R., McGregor, J. L., Lee, D. K., Wang, W. C., Ding, Y., & Kimura, F. (2004). Regional climate modeling: Progress, challenges, and prospects. *Journal of the Meteorological Society of Japan*, *82*(6), 1599–1628. https://doi.org/10.2151/jmsj.82.1599